

# A nonlinear global approach to scale-model aircraft path following control

Jean-Marie Kai, Tarek Hamel and Claude Samson

**Abstract**—This paper addresses the path following control problem for scale-model fixed-wing aircraft. Kinematic guidance and dynamic control laws are developed within a single coherent framework that exploits a simple generic model of aerodynamics forces acting on the aircraft and applies to almost all regular 3D paths. The proposed control solutions are derived on the basis of theoretical stability and convergence analyses. They are complemented by addressing several practical issues, and validated via realistic hardware-in-the-loop simulations.

## I. INTRODUCTION

During the last two decades important progress has been made in the development of advanced methods for motion control of autonomous Unmanned Aerial Vehicles (UAVs). The commercial landscape of these vehicles is characterised by a plethora of small start-up companies proposing an increasing variety of devices for various applications such as power lines inspection, data collecting, crops monitoring, real estate use of aerial photographs, etc. This rapidly growing market has in turn boosted research studies in the field of UAVs, particularly from the Systems and Control community, with specific control strategies developed in relation to different classes of aerial vehicles, as exemplified by scale-model airplanes, quadrotors and, more recently, tail-sitters. A typical aerial vehicle is an underactuated dynamic system with six main degrees of freedom (for the position and orientation of the vehicle's main body) and usually four (sometimes three) independent control inputs, i.e. a thrust force along the main direction of the vehicle, and three (or only two) control torques for body orientation modification. Associated motion control problems are commonly classified into two sub-categories, namely *trajectory tracking* and *path following*.

Trajectory tracking refers to the problem of stabilising a time-parametrised reference position trajectory. It is best adapted to highly manoeuvrable Vertical-Take-Off-and-Landing (VTOL) vehicles (quadrotors, helicopters, ducted-fans) [11], [14], [17], [23], convertible vehicles (tail-sitters in particular) [28] and acrobatic aircraft [26] whose positions have to be precisely and timely monitored near hovering. Its applicability to fixed-wing aircraft, although possible [12], [24], is more limited because the position-timing issue for cruising vehicles is less essential than following a pre-planned path with a given (possibly high) velocity needed

for the production of strong air-lift forces on profiled wings that dramatically reduce energy expenditure.

Path-following refers to the problem of stabilising a desired forward velocity and of zeroing the "distance" between the vehicle position and a desired geometric path. This "distance" can be characterized by the mathematical distance between a specific point located on the vehicle body and the orthogonal projection of this point onto the path [1], [18], [25], or by considering some variant characterization to avoid the orthogonal projection non-uniqueness issue in some particular situations [6], [21]. The path itself may be attached to a frame that is moving with respect to some fixed inertial frame [20]. Path following control has become a central feature of any advanced automated flight control system. It can be used for waypoints navigation, to fly a programmed course [1], [6], [18], and for a landing approach with a given glide slope [5]. It is commonly decomposed into sub-problems, namely guidance (sometimes termed as guidance-based control), velocity control, and attitude control. Guidance essentially consists in determining the desired heading direction for the aircraft given a path to follow [18], and involves body kinematic equations only. It is mostly independent of the aircraft characteristics and is usually associated with the notion of outer-loop control. By contrast, velocity and attitude controls take into account the specificities of the aircraft and of aerodynamic reaction forces that influence its dynamics. These lower level control tasks are associated with the notion of inner-loop control. Automatic monitoring of the aircraft velocity is commonly done via thrust production and is sometimes called auto-throttle control. Automatic monitoring of the aircraft attitude (or orientation) is in charge, via the production of torques, of making the actual aircraft heading direction converge to the direction specified at the guidance level and is typically performed by modifying the orientation angles of the aircraft control surfaces. For this latter task three-axis autopilots monitor angles of the aircraft ailerons (for roll motion), elevator(s) (for pitch motion), and rudder(s) (for yaw motion). Less sophisticated two-axis autopilots monitor roll and pitch motions only. The aforementioned separation between kinematic guidance and dynamic velocity and attitude control is conceptually attractive and convenient, all the more so that imprecise knowledge of aerodynamic forces acting on the aircraft dynamics constitutes the main source of difficulty for the design of robust controllers. Inner-loop controllers have historically, and to these days, been essentially designed on the basis of linearised modelled dynamic equations about so-called *trim* trajectories (for which the aircraft longitudinal

J.M. Kai and T. Hamel are with I3S, Université Côte d'Azur, CNRS, Sophia Antipolis, France, [kai\(thamel\)@i3s.unice.fr](mailto:kai(thamel)@i3s.unice.fr).

C. Samson (corresponding author) is with INRIA and I3S UCA-CNRS, Sophia Antipolis, France, [claude.samson@inria.fr](mailto:claude.samson@inria.fr), [csamson@i3s.unice.fr](mailto:csamson@i3s.unice.fr).

and angular velocities are constant) with attack and bank angles often taken as intermediary control variables [3], [27]. They are also reported in all major flight dynamics textbooks and, for this reason, are often taken for granted in path following studies that focus only on the simpler generic guidance part of the problem. Among the most advanced ones let us cite, for instance, those based on linear control techniques combined with gain scheduling [7], feedback linearisation combined with LQ control [8], or Linear Parameter Varying (LPV) modelling and control [9], [16].

In the present paper we propose a nonlinear control approach that encompasses within a single framework the different steps involved in aircraft path following control, i.e. guidance, velocity control and attitude control. This approach offers an alternative to current state-of-the-art automated flight solutions, and also to the Total Energy Control approach [2], [13] centred on the aircraft velocity/altitude monitoring, which has gained popularity in the field of small fixed-wing UAV control through its implementation on several open-source autopilot simulation packages. More specifically, the proposed control design methodology exploits a simple model of aerodynamical forces applied to the vehicle that is both representative of the physics underlying the creation of the environmental forces and sufficiently simple to lend itself to control design and analysis. It complements our previous work devoted to the trajectory tracking problem [12], [23] and involves three stages: i) thrust monitoring of the aircraft velocity, ii) design of a kinematic guidance vector yielding convergence to the desired path with the pre-specified route direction, and iii) determination of a desired body frame whose asymptotic stabilisation yields a balanced flight, i.e. sideslip angle zeroing, and convergence of the aircraft heading vector to the previously defined guidance vector. This control methodology originally assumes that the orientation dynamics is fully-actuated. However we show that it also applies, modulo minor adaptations, to aircraft possessing only two orientation control axes, i.e. either pitch-and-roll or pitch-and-yaw, provided that the aircraft is equipped with a rear vertical stabiliser and, for the pitch-and-yaw configuration, with a main wing dihedral.

The paper is organized as follows. Section II recalls the equations of motion of an aircraft, presents the model used for the aerodynamic forces acting on an aircraft, and specifies the control variables used for a *generic* control design that does not depend on specific aircraft actuation means. Section III first recalls the general control objectives associated with the path following problem and some useful relations related to the calculation of the distance between the aircraft and the desired path. The three aforementioned control design stages are subsequently detailed, yielding control laws that are theoretically justified via stability and convergence analyses. Assumptions under which exponential stability is achieved are then particularized and discussed in the common cases of straight and circular paths. Complementary practical issues, namely i) the extension of the control design to curves defined w.r.t. a translating frame, ii) its adaptation to two-axis

autopilots, iii) the determination of control surfaces angles from previously determined desired body angular velocity, and iv) the monitoring of thrust limitations and attack angle for stall avoidance, are addressed in Section IV. Hardware-in-the-loop simulation results involving a scale-model aircraft and challenging reference paths, with large initial tracking errors, imposed positive thrust, and air-velocity measurement approximations, purposely introduced to test the control performance and its robustness, are reported in Section V. Concluding remarks and a short list of possible extensions of this work are given in the last Section VI.

## II. CONTROL MODEL

### A. Notation

Throughout the paper,  $\mathbf{E}^3$  denotes the 3D Euclidean vector space and vectors in  $\mathbf{E}^3$  are denoted with bold letters. Unless specified otherwise the associated reference frame is the inertial frame with respect to (w.r.t.) which the aircraft position is defined. Inner and cross products in  $\mathbf{E}^3$  are denoted by the symbols  $\cdot$  and  $\times$  respectively. The following notation is used.

- When  $x \in \mathbb{R}^n$  (resp.  $\mathbf{x} \in \mathbf{E}^3$ )  $|x|$  (resp.  $|\mathbf{x}|$ ) denotes the Euclidean norm of  $x$  (resp.  $\mathbf{x}$ ).
- $\bar{s}at^\Delta(y)$  ( $\Delta > 0$ ,  $y \in \mathbb{R}^n$ ) denotes a twice differentiable adaptation, with bounded derivatives, of the classical vector-valued saturation function  $sat^\Delta(y) = \min(1, \frac{\Delta}{|y|})y$ . More precisely  $\bar{s}at^\Delta(y) = \alpha^\Delta(|y|)y$  with  $\alpha^\Delta : [0, +\infty) \mapsto (0, 1]$  a decreasing twice differentiable function such that  $\alpha^\Delta(0) = 1$ ,  $\frac{d}{dx}\alpha^\Delta(0) = \frac{d^2}{dx^2}\alpha^\Delta(0) = 0$ ,  $\alpha^\Delta(x) \leq \frac{\Delta}{x}$ ,  $\lim_{x \rightarrow +\infty}(\alpha^\Delta(x)x) = \Delta$ . A typical example is  $\alpha^\Delta(x) = \frac{\Delta}{x} \tanh(\frac{x}{\Delta})$ . From these definitions  $\bar{s}at^\Delta(y) \approx y$  when  $|y|$  is small and  $|\bar{s}at^\Delta(y)| \leq \Delta$ ,  $\forall y$ .
- $G$  denotes the aircraft center of mass (CoM);
- $\mathcal{I} = \{O; \mathbf{v}_0, \mathbf{j}_0, \mathbf{k}_0\}$  is an inertial frame;
- $\mathcal{B} = \{G; \mathbf{v}, \mathbf{j}, \mathbf{k}\}$  is an aircraft-fixed frame;
- $\boldsymbol{\omega}$  is the angular velocity of  $\mathcal{B}$  w.r.t.  $\mathcal{I}$ , i.e.

$$\frac{d}{dt}(\mathbf{v}, \mathbf{j}, \mathbf{k}) = \boldsymbol{\omega} \times (\mathbf{v}, \mathbf{j}, \mathbf{k}) \quad (1)$$

- $m$  is the body mass;
- $\mathbf{v}$  is the CoM velocity w.r.t. the inertial frame;
- $\mathbf{a}$  is the CoM acceleration w.r.t. the inertial frame;
- $\mathbf{g} = g_0 \mathbf{k}_0$  is the gravitational acceleration;
- $\mathbf{v}_w$  is the ambient wind velocity w.r.t.  $\mathcal{I}$ ;
- $\mathbf{v}_a = \mathbf{v} - \mathbf{v}_w$  is the aircraft air-velocity. The direction of  $\mathbf{v}_a$  in body frame can be characterized by two angles  $\alpha$  and  $\beta$  such that

$$\mathbf{v}_a = |\mathbf{v}_a|(\cos \alpha(\cos \beta \mathbf{v} + \sin \beta \mathbf{j}) + \sin \alpha \mathbf{k}) \quad (2)$$

- The coordinate vector of any  $\boldsymbol{\xi} \in \mathbf{E}^3$  w.r.t. the body-fixed frame  $\mathcal{B}$  is denoted by the ordinary letter  $\xi$ , i.e.  $\boldsymbol{\xi} = \xi_1 \mathbf{v} + \xi_2 \mathbf{j} + \xi_3 \mathbf{k}$  with  $\xi = [\xi_1, \xi_2, \xi_3]^\top$ .

In the case of an airplane, and with a proper choice of the body frame unit vectors,  $\alpha = \arcsin(v_{a,3}/|\mathbf{v}_a|)$  and  $\beta = \arctan(v_{a,2}/v_{a,1})$  denote the attack angle and sideslip angle respectively. This definition slightly differs from the

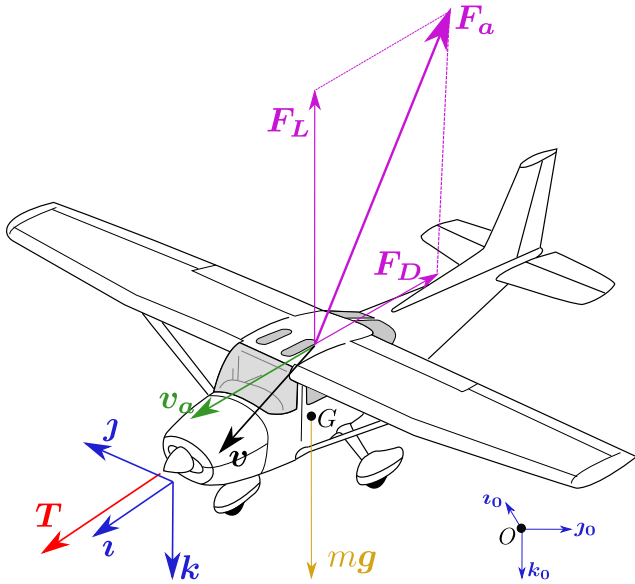


Fig. 1. Frames and forces

one classically used in aeronautics but the two definitions are locally equivalent for small angles. Note also that, like any parametrization of the unit sphere by two angles, this representation is not uniquely defined everywhere. More precisely  $\beta$  cannot be defined by continuity at  $\alpha = \pm\pi/2$ .

### B. Aerodynamic forces

The resultant aerodynamic force  $\mathbf{F}_a$  applied to a rigid body moving with air-velocity  $\mathbf{v}_a$  is traditionally decomposed into the sum of a drag force  $\mathbf{F}_D$  along the direction of  $\mathbf{v}_a$  and a lift force  $\mathbf{F}_L$  perpendicular to this direction, i.e.

$$\mathbf{F}_a = \mathbf{F}_D + \mathbf{F}_L \quad (3)$$

The intensities of drag and lift forces are essentially proportional to  $|\mathbf{v}_a|^2$  modulo variations characterized by two dimensionless functions  $C_D$  and  $C_L$ , which depend in the first place on the orientation of  $\mathbf{v}_a$  w.r.t. the body, but also on the Reynolds number  $Re$  and Mach number  $M$ . These dimensionless functions are called the *aerodynamic characteristics* of the body, or *drag coefficient* and *lift coefficient* respectively. More precisely

$$\mathbf{F}_D = -\eta_a |\mathbf{v}_a| C_D \mathbf{v}_a, \quad \mathbf{F}_L = \eta_a |\mathbf{v}_a| C_L \mathbf{v}_a^\perp \quad (4)$$

with

- $\mathbf{v}_a^\perp$  some vector perpendicular to  $\mathbf{v}_a$  and such that  $|\mathbf{v}_a^\perp| = |\mathbf{v}_a|$ ,
- $\eta_a := \frac{\rho \Sigma}{2}$  with  $\rho$  the *free stream* air density, and  $\Sigma$  an area germane to the body shape.

Throughout the paper, we assume that the torque produced by the resultant aerodynamic force  $\mathbf{F}_a$  can, in practice, be overcome by a chosen control torque produced, for instance, by control surfaces. A common assumption in the flight control literature, when  $\alpha, \beta$  are well defined, is that the aerodynamic characteristics depend essentially on  $\alpha$  and  $\beta$  (i.e.  $C_D = C_D(\alpha, \beta)$  and  $C_L = C_L(\alpha, \beta)$ ). Accordingly, we

neglect here the dependence of the aerodynamic characteristics on the Reynolds and Mach numbers. This all the more justified in the case of scale-model aircraft evolving at nearly constant altitudes and at speeds much lower than the speed of sound.

### C. Body dynamics

We assume that the control inputs consist of a thrust force  $\mathbf{T} = T\mathbf{i}$  applied at  $G$ , with  $T$  the thrust intensity, and a torque vector  $\mathbf{\Gamma}$  that is essentially produced by the aircraft moving control surfaces. In other words we assume that the torque produced by these surfaces easily dominates the torque produced by fixed surfaces so that this latter torque can, in the first approximation, be omitted in the modelling equations of the aircraft. On the other hand, since moving surfaces are typically much smaller than fixed surfaces, the relative variation of the aerodynamic forces about the neutral positions of these surfaces is limited and can also be neglected in the first approximation. For the sake of simplification we further assume that the thrust direction  $\mathbf{i}$  is parallel to the aircraft zero-lift plane and that the corresponding propulsive force does not produce a significant torque. This direction thus represents the longitudinal motion direction of the aircraft. The unit vector  $\mathbf{j}$  can also be chosen parallel to the zero-lift plane. Being orthogonal to  $\mathbf{i}$  it represents the aircraft lateral motion direction. Under these assumptions and approximations, the aircraft dynamic equations are given by (1) complemented with the classical Newton-Euler equations:

$$m\mathbf{a} = m\mathbf{g} + \mathbf{F}_a + T\mathbf{i} \quad (5)$$

$$J\dot{\boldsymbol{\omega}} = -S(\boldsymbol{\omega})J\boldsymbol{\omega} + \mathbf{\Gamma} \quad (6)$$

with  $J$  the body inertia matrix, and  $\mathbf{\Gamma}$  the vector of coordinates of  $\mathbf{\Gamma}$  in the body frame. In view of Eq. (6),  $\boldsymbol{\omega}$  can be modified at will via the choice of the control torque  $\mathbf{\Gamma}$  so that one can consider the angular velocity  $\boldsymbol{\omega}$  as an intermediate control input. The corresponding physical assumption is that “almost” any desired angular velocity can be obtained after a short transient time. This is a standard “backstepping” assumption. Once it is made, the vehicle actuation consists in four input variables, namely, the thrust intensity  $T$  and the three components of  $\boldsymbol{\omega}$ . This assumption allows one to “eliminate” or, more precisely, postpone the complementary issue of producing a desired angular velocity via a torque  $\mathbf{\Gamma}$  that can be produced via various and specific physical means (control surfaces, in the case of a standard airplane). The body dynamics equations are then reduced to (1) and (5).

### D. Modelling of aerodynamic forces

To be usable for control design, the Newton equation (5) has to be complemented with a model of the resultant aerodynamic force  $\mathbf{F}_a$ . It is well known that the norm of aerodynamic forces are commensurate with the squared norm of the air-velocity so that one can safely assume that there exists two positive numbers  $c$  and  $d$  such that

$$|\mathbf{F}_a| < c + d|\mathbf{v}_a|^2 \quad (7)$$

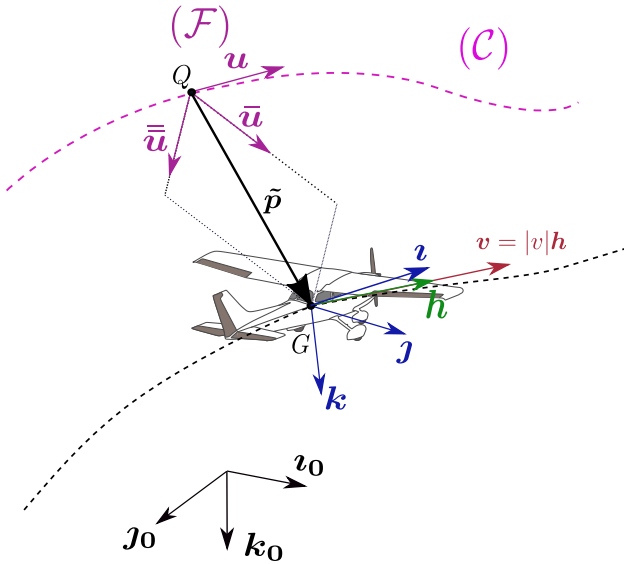


Fig. 2. Desired path and position errors

The model that we propose to use is:

$$\mathbf{F}_a = -(c_0 v_{a,1} \mathbf{v} + \bar{c}_0 v_{a,3} \mathbf{k}) |v_a| + v_{a,2} \mathbf{O}(v_a) \quad (8)$$

with  $c_0$  and  $c_1$  denoting positive numbers,  $\bar{c}_0 = c_0 + 2c_1$ , and  $\mathbf{O}(v_a)$  any Euclidean vector-valued function such that the ratio  $\frac{|\mathbf{O}(v_a)|}{|v_a|}$  is bounded. For instance, in [12] we have used  $\mathbf{O}(v_a) = -c_0 |v_a| \mathbf{j}$  for a model of a disc-shaped aircraft. Relation (8) is compatible with the assumed aircraft symmetry about the plane  $(G; \mathbf{v}, \mathbf{k})$ . Note that if the drag coefficient  $c_0$  were equal to zero then, in the case of zero sideslip angle ( $v_{a,2} = 0$ ), the resultant aerodynamic force would be orthogonal to the zero-lift plane with an amplitude proportional to  $\sin \alpha |v_a|^2$ . This model is also compatible with the previous relations (3) and (4). Indeed, one easily verifies that, in this case,  $v_a^\perp = \frac{|v_a|}{\cos \alpha} \mathbf{k} - \tan \alpha v_a$ ,  $C_D(\alpha) = (c_0 + 2c_1 \sin^2 \alpha) / \eta_a$ , and  $C_L(\alpha) = c_1 \sin 2\alpha / \eta_a$ . For small attack angles  $|\alpha|$  the drag coefficient  $C_D$  is thus approximately equal to  $\frac{c_0}{\eta_a}$  and the lift coefficient  $C_L$  is approximately proportional to the attack angle with the coefficient of proportionality given by  $\frac{2c_1}{\eta_a}$ . This is coherent with experimental data performed on a variety of wing profiles and axisymmetric bodies [23]. However, for lift-optimized wing profiles this model fails to account for stall phenomena occurring at large attack angles. A way to tentatively overcome this shortcoming consists in changing the coefficients  $c_0$  and  $c_1$  beyond the stall angle.

### III. CONTROL

#### A. Objectives and useful relations

Consider a three-times differentiable curve  $\mathcal{C}$  in 3D-space parametrized by its curvilinear abscissa  $s$  and, at the point  $Q(s)$  on this path, an associated *parallel transport frame*  $\mathcal{F} = \{Q; \mathbf{u}, \bar{\mathbf{u}}, \bar{\bar{\mathbf{u}}}\}$  with  $\mathbf{u}$  the vector tangent to the path  $\mathcal{C}$  at the point  $Q$ . An advantage of a parallel transport frame over the more conventional Frénet frame is that it is (continuously) well-defined at points where the path curvature vanishes. It does not suffer from ambiguity and

sudden orientation changes when the curves straightens out [4] [10]. Its (relative) drawback is that it is not defined from the sole curve characteristics (curvature and torsion). More precisely, it is uniquely defined only once the vectors  $\bar{\mathbf{u}}$  and  $\bar{\bar{\mathbf{u}}}$  are (arbitrarily) chosen at some point on the curve. The corresponding variational frame equations are

$$\frac{d}{ds} \bar{\mathbf{u}} = -\gamma_1 \mathbf{u}; \quad \frac{d}{ds} \bar{\bar{\mathbf{u}}} = -\gamma_2 \mathbf{u}; \quad \frac{d}{ds} \mathbf{u} = \gamma_1 \bar{\mathbf{u}} + \gamma_2 \bar{\bar{\mathbf{u}}} \quad (9)$$

With this formalism any smooth curve is characterized by an initial point at  $s = 0$ , the choice of a parallel transport frame at this point, and the functions  $\gamma_1(s)$  and  $\gamma_2(s)$ . These functions are themselves related to the curve curvature  $\kappa$  and torsion  $\tau$  according to  $\kappa = \sqrt{\gamma_1^2 + \gamma_2^2}$  and  $\tau = \frac{d}{ds}(\arctan(\frac{\gamma_2}{\gamma_1}))$ . For instance,  $(\gamma_1 = 0, \gamma_2 = 0)$  in the case of a straight line,  $(\gamma_1 = \frac{1}{r}, \gamma_2 = 0)$  in the case of a circle with radius  $r$ , and  $(\gamma_1(s) = \kappa \cos(\tau s + c), \gamma_2(s) = \kappa \sin(\tau s + c))$  –with  $c$  denoting a constant depending on the choice of the initial frame– in the case of a helix with constant curvature and torsion.

Given a curve  $\mathcal{C}$ , the path following control objective consists in i) stabilising the aircraft speed at a desired value, and ii) having the aircraft converge to the curve and then follow it. Let  $\mathbf{p}$  denote the aircraft CoM position and  $\mathbf{q}$  denote the position of the point  $Q$  on the curve closest to  $G$ . Depending on the curve, this point can be always unique (as in the case of a straight line) or only locally unique, depending on the position of the aircraft w.r.t. the curve (as, for instance, in the case of a circle for which uniqueness is granted provided that  $G$  does not belong to the circle axis passing through the origin and perpendicular to the circle's plane). Define the position error vector  $\tilde{\mathbf{p}} =: \mathbf{p} - \mathbf{q}$ , and let  $v^* \in \mathbb{R}^+$  denote the desired magnitude of the aircraft velocity. A way to achieve the previously evoked control objectives consists in stabilising  $|v| - v^*$  and  $\tilde{\mathbf{p}}$  at zero.

By definition of  $Q$  (point on the curve closest to  $G$ ) the vector  $\tilde{\mathbf{p}}$  is perpendicular to the tangent to the curve at  $Q$ . It thus belongs to the plane  $\{Q; \bar{\mathbf{u}}, \bar{\bar{\mathbf{u}}}\}$ . Let  $y = [y_1, y_2]^\top \in \mathbb{R}^2$  denote the vector of non-zero coordinates of  $\tilde{\mathbf{p}}$  expressed in the basis of the parallel transport frame  $\mathcal{F} = \{Q; \mathbf{u}, \bar{\mathbf{u}}, \bar{\bar{\mathbf{u}}}\}$ , i.e.  $\tilde{\mathbf{p}} = y_1 \bar{\mathbf{u}} + y_2 \bar{\bar{\mathbf{u}}}$  with  $y_1 =: \tilde{\mathbf{p}} \cdot \bar{\mathbf{u}}$  and  $y_2 =: \tilde{\mathbf{p}} \cdot \bar{\bar{\mathbf{u}}}$ . The convergence of  $\tilde{\mathbf{p}}$  to zero is equivalent to the convergence of  $y$  to zero. With  $\tilde{\mathbf{p}}$  taken as a Euclidean vector w.r.t. the reference frame  $\mathcal{F}$  one can make this vector converge to zero by considering its variations w.r.t. to this frame. From now on we will use the notation  $\dot{\tilde{\mathbf{p}}}_{\mathcal{F}}$ ,  $\ddot{\tilde{\mathbf{p}}}_{\mathcal{F}}$  and  $\ddot{\tilde{\mathbf{p}}}_{\mathcal{F}}$  when the vector  $\tilde{\mathbf{p}}$  and its derivatives are taken as Euclidean vectors in the reference frame  $\mathcal{F}$ . One has

$$\dot{\tilde{\mathbf{p}}} = \frac{d}{dt} \vec{OG} - \frac{d}{dt} \vec{OQ} = \mathbf{v} - \dot{s} \mathbf{u} \quad (10)$$

and

$$\dot{\tilde{\mathbf{p}}}_{\mathcal{F}} = \dot{y}_1 \bar{\mathbf{u}} + \dot{y}_2 \bar{\bar{\mathbf{u}}}$$

with

$$\begin{aligned} \dot{y}_1 &= \dot{\tilde{\mathbf{p}}} \cdot \bar{\mathbf{u}} + \tilde{\mathbf{p}} \cdot \dot{\bar{\mathbf{u}}} \\ &= (\mathbf{v} - \dot{s} \mathbf{u}) \cdot \bar{\mathbf{u}} + \tilde{\mathbf{p}} \cdot (-\gamma_1 \mathbf{u}) \\ &= \mathbf{v} \cdot \bar{\mathbf{u}} \end{aligned}$$

$$\begin{aligned}
\dot{y}_2 &= \dot{\tilde{p}} \cdot \bar{\mathbf{u}} + \tilde{p} \cdot \dot{\bar{\mathbf{u}}} \\
&= (\mathbf{v} - \dot{\mathbf{s}}\mathbf{u}) \cdot \bar{\mathbf{u}} + \tilde{p} \cdot (-\gamma_2 \mathbf{u}) \\
&= \mathbf{v} \cdot \bar{\mathbf{u}}
\end{aligned}$$

Therefore  $\dot{y} = [\mathbf{v} \cdot \bar{\mathbf{u}}, \mathbf{v} \cdot \bar{\mathbf{u}}]^\top$ . This relation may also be written as

$$\begin{aligned}
\dot{\tilde{p}}_{\mathcal{F}} &= (\mathbf{v} \cdot \bar{\mathbf{u}}) \bar{\mathbf{u}} + (\mathbf{v} \cdot \bar{\mathbf{u}}) \dot{\bar{\mathbf{u}}} \\
&= \Pi_{\mathbf{u}} \mathbf{v}
\end{aligned} \tag{11}$$

with  $\Pi_{\mathbf{u}}$  denoting the operator of projection on the plane orthogonal to  $\mathbf{u}$ . Forming the second time-derivative of  $\tilde{p}_{\mathcal{F}}$  yields

$$\begin{aligned}
\ddot{\tilde{p}}_{\mathcal{F}} &= \frac{d}{dt}(\mathbf{v} \cdot \bar{\mathbf{u}}) \bar{\mathbf{u}} + \frac{d}{dt}(\mathbf{v} \cdot \bar{\mathbf{u}}) \dot{\bar{\mathbf{u}}} \\
&= (\mathbf{a} \cdot \bar{\mathbf{u}} + \mathbf{v} \cdot \dot{\bar{\mathbf{u}}}) \bar{\mathbf{u}} + (\mathbf{a} \cdot \bar{\mathbf{u}} + \mathbf{v} \cdot \dot{\bar{\mathbf{u}}}) \dot{\bar{\mathbf{u}}}
\end{aligned}$$

with  $\dot{\bar{\mathbf{u}}} = -\gamma_1 \dot{\mathbf{s}}\mathbf{u}$  and  $\dot{\bar{\mathbf{u}}} = -\gamma_2 \dot{\mathbf{s}}\mathbf{u}$ . Therefore  $\dot{y} = [\mathbf{a} \cdot \bar{\mathbf{u}} - \dot{\mathbf{s}}(\mathbf{u} \cdot \mathbf{v})\gamma_1 \bar{\mathbf{u}}, \mathbf{a} \cdot \bar{\mathbf{u}} - \dot{\mathbf{s}}(\mathbf{u} \cdot \mathbf{v})\gamma_2 \bar{\mathbf{u}}]^\top$ , and this relation may also be written as

$$\begin{aligned}
\ddot{\tilde{p}}_{\mathcal{F}} &= (\mathbf{a} \cdot \bar{\mathbf{u}}) \bar{\mathbf{u}} + (\mathbf{a} \cdot \bar{\mathbf{u}}) \dot{\bar{\mathbf{u}}} - \dot{\mathbf{s}}(\mathbf{u} \cdot \mathbf{v})(\gamma_1 \bar{\mathbf{u}} + \gamma_2 \dot{\bar{\mathbf{u}}}) \\
&= \Pi_{\mathbf{u}} \mathbf{a} - \dot{\mathbf{s}}(\mathbf{u} \cdot \mathbf{v})(\gamma_1 \bar{\mathbf{u}} + \gamma_2 \dot{\bar{\mathbf{u}}})
\end{aligned} \tag{12}$$

This latter relation calls for the calculation of  $\dot{\mathbf{s}}$ . We have already established that

$$\begin{aligned}
\dot{\mathbf{s}}\mathbf{u} &= \mathbf{v} - \dot{\tilde{p}} \\
&= \mathbf{v} - (\dot{\tilde{p}}_{\mathcal{F}} + y_1 \dot{\bar{\mathbf{u}}} + y_2 \dot{\bar{\mathbf{u}}}) \\
&= \mathbf{v} - \dot{\tilde{p}}_{\mathcal{F}} + (\gamma_1 y_1 + \gamma_2 y_2) \dot{\mathbf{s}}\mathbf{u}
\end{aligned}$$

The scalar product of both members of the previous equality with  $\mathbf{u}$  yields

$$\dot{\mathbf{s}} = \frac{(\mathbf{u} \cdot \mathbf{v})}{1 - \gamma_1 y_1 - \gamma_2 y_2} \tag{13}$$

Using this relation in (12) yields

$$\begin{aligned}
\ddot{\tilde{p}}_{\mathcal{F}} &= \Pi_{\mathbf{u}} \mathbf{a} + \boldsymbol{\eta} \\
\boldsymbol{\eta} &:= -\frac{(\mathbf{u} \cdot \mathbf{v})^2}{1 - \gamma_1 y_1 - \gamma_2 y_2} (\gamma_1 \bar{\mathbf{u}} + \gamma_2 \dot{\bar{\mathbf{u}}})
\end{aligned} \tag{14}$$

### B. Control design

A central quantity involved in the control of any aircraft is the velocity vector  $\mathbf{v} = |\mathbf{v}|\mathbf{h}$  with  $\mathbf{h} := \frac{\mathbf{v}}{|\mathbf{v}|}$  denoting the *heading vector* that specifies the direction of displacement of the aircraft and  $|\mathbf{v}|$  the inertial speed. In the case of the path following problem here addressed the decomposition of  $\mathbf{v}$  into the product of  $|\mathbf{v}|$  by  $\mathbf{h}$  is all the more justified that convergence to the desired path can be performed at various speeds with the same heading policy and, *vice versa*, that changing the heading policy does not imply modifying the aircraft speed. Decoupling the  $|\mathbf{v}|$  control problem from the control of  $\mathbf{h}$  is also natural because these problems essentially involve separate physical inputs: monitoring of  $|\mathbf{v}|$  is done via thrust adaptation, i.e. via the control input  $T$ , whereas monitoring of  $\mathbf{h}$  is performed via the control of the aircraft attitude, i.e. via the control input  $\omega$ . The task of a human pilot is facilitated by this decoupling, just as in the case of car-driving. In order to avoid useless theoretical complications, we assume from now on that the thrust  $T$  applied to the aircraft is bounded. Assuming also that the wind velocity is bounded, this in turn implies, by virtue of energy dissipation in the air, which increases roughly like

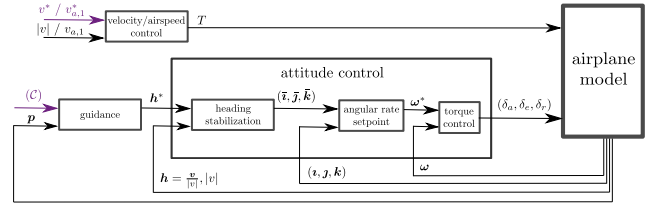


Fig. 3. Control block diagram

$|v|^2$  (the term  $-c_0 v_{a,1}|v_a|$  in the model contributes to this dissipation), that  $|v|$  is itself bounded.

The proposed control design involves the interconnection of three stages see Fig. 3, namely i) velocity monitoring via thrust adaptation, ii) desired heading vector determination (guidance), and iii) attitude control for the balanced flight stabilisation of the desired heading vector. These three stages are detailed next.

1) *Velocity control via thrust adaptation*: The model of aerodynamic forces (8) may also be written as

$$\mathbf{F}_a = -\bar{c}_0 |v_a| \mathbf{v}_a + 2c_1 v_{a,1} |v_a| \mathbf{i} + m v_{a,2} \bar{O}(\mathbf{v}_a) \tag{15}$$

with  $\bar{O}(\mathbf{v}_a) = \frac{1}{m}(O(\mathbf{v}_a) + \bar{c}_0 |v_a| \mathbf{j})$ . Combining this relation with (5) yields

$$\mathbf{a} = \bar{\mathbf{g}} + \frac{\bar{T}}{m} \mathbf{i} + v_{a,2} \bar{O}(\mathbf{v}_a) \tag{16}$$

with

$$\bar{\mathbf{g}} := \mathbf{g} - \frac{\bar{c}_0}{m} |v_a| \mathbf{v}_a \tag{17}$$

and

$$\bar{T} := T + 2c_1 v_{a,1} |v_a| \tag{18}$$

Let  $v^*$  denote the desired value of  $|v|$  and define  $err := |v| - v^*$ . By using (16) one finds that

$$\frac{d}{dt} err = \bar{\mathbf{g}} \cdot \mathbf{h} + (\mathbf{i} \cdot \mathbf{h}) \frac{\bar{T}}{m} - \dot{v}^* + v_{a,2} \bar{O}(\mathbf{v}_a) \cdot \mathbf{h} \tag{19}$$

This relation in turn suggests to set

$$\bar{T} = m(-\bar{\mathbf{g}} \cdot \mathbf{h} + \dot{v}^* - k_{T,1} err - k_{T,2} I_{err}) / (\mathbf{i} \cdot \mathbf{h}) \tag{20}$$

with  $k_{T,1}$  and  $k_{T,2}$  denoting positive gains and  $I_{err}$  some bounded integral of the velocity error  $err$ . This Proportional-Integral (PI) feedback controller complemented with a pre-compensation term is well defined if  $\mathbf{i} \cdot \mathbf{h} \neq 0$  (a nominally satisfied condition on which we will come back further) and yields the closed-loop equation

$$\frac{d}{dt} err = -k_{T,1} err - k_{T,2} I_{err} + v_{a,2} \bar{O}(\mathbf{v}_a) \cdot \mathbf{h}$$

from which the exponential convergence of  $err$  to zero follows provided that the lateral velocity component  $v_{a,2}$  itself converges to zero exponentially, i.e. provided that a "balanced" flight with zero sideslip angle is achieved. How to control the aircraft attitude so as to achieve this latter property is addressed later on via the control of the aircraft attitude. In practice, since no division by zero is allowed, division by  $\mathbf{i} \cdot \mathbf{h}$  can be replaced by the multiplication by  $|\mathbf{v}|(\mathbf{i} \cdot \mathbf{v}) / ((\mathbf{i} \cdot \mathbf{v})^2 + \epsilon)$  with  $\epsilon$  denoting a small positive number.

This rule applies to any division by a term  $x$  that may cross zero. Note also that the gains  $k_{T,1}$  and  $k_{T,2}$  do not have to be constant. In particular they may be of the form  $k_{T,j} = |\mathbf{v}|k_{T,j}^0$  with  $k_{T,j}^0 > 0$  so as to avoid numerical problems in the eventuality where  $|\mathbf{v}|$  becomes very small. Note finally that an approximation of the above controller consists in exploiting the fact that the aircraft angle of attack is nominally small, which is equivalent to assuming that the vectors  $\mathbf{v}$  and  $\mathbf{h}$  are nearly aligned. With this assumption, and neglecting the wind velocity one has  $v_{a,1} = \mathbf{v} \cdot \mathbf{v} \approx \mathbf{v} \cdot \mathbf{h} = |v|$  and  $\mathbf{v} \cdot \mathbf{h} \approx 1$  so that, after simple calculations, relation (20) yields

$$T \approx T^* - m(k_{T,1}err + k_{T,2}I_{err}) \quad (21)$$

with  $T^* := -m\mathbf{g} \cdot \mathbf{h} + c_0|v|^2 + m\dot{v}^*$ . A pure PI controller, i.e. without the pre-compensation term  $T^*$  and with large enough gains, may also in practice be sufficient to monitor the aircraft speed satisfactorily. Note that the integral action is not only useful to compensate for the absence of the pre-compensation term, but also to compensate for the imperfect knowledge of the physically applied thrust.

Alternatively, instead of  $|v|$  one may wish to monitor the air-velocity in the direction of  $\mathbf{v}$ , i.e. the component  $v_{a,1} = \mathbf{v}_a \cdot \mathbf{v}$ , which can be measured, for instance, with a pitot tube. Define now the velocity error  $err := v_{a,1} - v^*$ . Using (16) the time-derivative of  $err$  satisfies the relation

$$\begin{aligned} \frac{d}{dt}err &= \frac{d}{dt}((\mathbf{v} - \mathbf{v}_w) \cdot \mathbf{v}) - \dot{v}^* \\ &= (\mathbf{a} - \dot{\mathbf{v}}_w) \cdot \mathbf{v} + \boldsymbol{\omega} \cdot (\mathbf{v} \times \mathbf{v}_a) - \dot{v}^* \\ &= (\mathbf{g} - \dot{\mathbf{v}}_w) \cdot \mathbf{v} + \boldsymbol{\omega} \cdot (\mathbf{v} \times \mathbf{v}_a) - \frac{c_0}{m}|v_a|v_{a,1} \\ &\quad - \dot{v}^* + \frac{T}{m} + v_{a,2}\bar{O}(\mathbf{v}_a) \cdot \mathbf{v} \end{aligned}$$

Assuming that  $v_{a,2}$  converges exponentially to zero (balanced flight), exponential convergence of  $v_{a,1} - v^*$  to zero is then obtained by setting

$$T = T^* - m(k_{T,1}err + k_{T,2}I_{err}) \quad (22)$$

with  $T^* := -m((\mathbf{g} - \dot{\mathbf{v}}_w) \cdot \mathbf{v} + \boldsymbol{\omega} \cdot (\mathbf{v} \times \mathbf{v}_a) - \frac{c_0}{m}|v_a|v_{a,1} - \dot{v}^*)$ ,  $k_{T,1}$  and  $k_{T,2}$  denoting positive gains, and  $I_{err}$  some bounded integral of  $err$ . As in the previous case the simple PI controller obtained by omitting the pre-compensation term  $T^*$  may be sufficient in practice to bring and maintain  $err$  close to zero.

2) *Desired heading vector determination (guidance):* By viewing the aircraft as a point moving in 3D-space with a given velocity  $|v|$  the problem is to determine a desired heading direction  $\mathbf{h}^*$  that yields the convergence of this point to the desired path and ensures that the point moves thereafter along the path with the desired direction given by  $\pm \mathbf{u}$ , i.e. such that  $\mathbf{h}^*$  converges to  $sign_{v_u} \mathbf{u}$  with  $sign_{v_u}$  chosen in advance and equal to either 1 or  $-1$ . There are obviously a multitude of solutions to this problem, a certain number of which have been reported in the literature [6] [22] [20]. The solution that we propose here consists in setting

$$\mathbf{h}^* = \sin(\theta_h)\mathbf{l} + \cos(\theta_h)sign_{v_u} \mathbf{u} \quad (23)$$

with  $\mathbf{l}$  denoting some unit vector orthogonal to  $\mathbf{u}$  and  $\theta_h$  an angle depending on the position error  $\tilde{\mathbf{p}}$  and converging to

zero when  $|\tilde{\mathbf{p}}|$  tends to zero. For instance, a simple possible choice for  $\mathbf{l}$  and  $\theta_h$  is

$$\bar{y} := k_1 Ds\bar{a}t^{\Delta_h}(y)/|v| \quad (24a)$$

$$\theta_h := \arctan(|\bar{y}|/\sqrt{1-|\bar{y}|^2}) \quad (24b)$$

$$\mathbf{l} := -\frac{\bar{y}_1\bar{\mathbf{u}} + \bar{y}_2\bar{\bar{\mathbf{u}}}}{|\bar{y}|} \quad (24c)$$

with  $D = \text{diag}\{d_1, d_2\}$  a diagonal matrix with  $d_i \in (0, 1]$  ( $i = 1, 2$ ),  $\Delta_h := \frac{\mu|v|}{k_1 \max(d_1, d_2)}$ ,  $\mu \in (0, 1)$ , and  $k_1$  a positive gain. Note that  $|\bar{y}| < 1$  so that  $\theta_h$  is well defined and belongs to  $[0, \pi/2)$ . Note also that  $\sin(\theta_h) = |\bar{y}| \leq \mu$  so that the term  $\sin(\theta_h)\mathbf{l}$  entering the expression of  $\mathbf{h}^*$  is always well defined. Moreover, if  $d_1 = d_2$  then  $\sin(\theta_h)$  tends to  $\mu$  when  $|y|$  tends to infinity. Therefore, in this case  $\arcsin(\mu)$  characterizes the angle of incidence of the desired heading direction w.r.t. the tangent to the desired path at the point  $Q$  when the aircraft is far from the path. The usefulness of choosing  $d_1 \neq d_2$  is related to the possibility of imposing different upper bounds upon  $|\dot{y}_1|$  and  $|\dot{y}_2|$ , a feature which may be useful to separate the rates of convergence along the directions  $\bar{\mathbf{u}}$  and  $\bar{\bar{\mathbf{u}}}$  and limit the rate of descent or of climb of the aircraft when, for instance,  $\bar{\mathbf{u}}$  is a vertical vector as in the case of a linear or circular horizontal path.

The following proposition summarizes the stability and convergence properties associated with this desired heading direction.

**Proposition 1** *If  $\mathbf{h} = \mathbf{h}^*$  with  $\mathbf{h}^*$  given by (23) and (24), then  $(y, \dot{y}) = (0, 0)$  is globally asymptotically (locally exponentially) stable and  $\mathbf{h}$  tends to  $sign_{v_u} \mathbf{u}$ . Moreover  $|\dot{y}(t)|$  is upper bounded by  $\mu|v|$  and  $|\dot{y}_i(t)|$  is upper bounded by  $\frac{d_i}{\max(d_1, d_2)}\mu|v|$  ( $i = 1, 2$ ).*

**Proof:** When  $\mathbf{h} = \mathbf{h}^*$  the variation of  $\tilde{\mathbf{p}}_{\mathcal{F}}$  is given by

$$\begin{aligned} \dot{\tilde{\mathbf{p}}}_{\mathcal{F}} &= \Pi_{\mathbf{u}} \mathbf{v} = |v|\Pi_{\mathbf{u}} \mathbf{h}^* \\ &= |v|\Pi_{\mathbf{u}} \sin(\theta_h)\mathbf{l} \\ &= |v||\bar{y}|\mathbf{l} \\ &= -|v|(\bar{y}_1\bar{\mathbf{u}} + \bar{y}_2\bar{\bar{\mathbf{u}}}) \end{aligned}$$

and, since  $\dot{\tilde{\mathbf{p}}}_{\mathcal{F}} = \dot{y}_1\bar{\mathbf{u}} + \dot{y}_2\bar{\bar{\mathbf{u}}}$ , it comes that  $\dot{y} = -|v|\bar{y} = -k_1 Ds\bar{a}t^{\Delta_h}(y)$ . The announced upper bounds of  $|\dot{y}(t)|$  and  $|\dot{y}_i(t)|$  ( $i = 1, 2$ ) follow directly from this latter equality. The convergence of  $y$  and  $\dot{y}$  to zero then follows from re-writing the previous equality as  $\dot{y}_i = -k_1 d_i \alpha^{\Delta_h}(|y|)y_i$  ( $i = 1, 2$ ), so that  $0.5 \frac{d}{dt}y_i^2 = -k_1 d_i \alpha^{\Delta_h}(|y|)y_i^2 (\leq 0)$ . Finally the exponential stability of  $(y, \dot{y}) = (0, 0)$  in the sense of Lyapunov is simply inherited from the non-saturated equation  $\dot{y} = -k_1 D y$  that holds when  $|y|$  is small. Finally, since  $|y|$  and thus  $|\bar{y}|$  tend to zero,  $\theta_h$  converges to zero and, in view of (23),  $\mathbf{h} (= \mathbf{h}^*)$  converges to  $sign_{v_u} \mathbf{u}$ .

**(end of proof).**

Any other guidance law  $\mathbf{h}^*$  yielding the same properties when  $\mathbf{h} = \mathbf{h}^*$ , i.e. exponential stability of  $(y, \dot{y}) = (0, 0)$  and convergence of  $\mathbf{h}^*$  to  $sign_{v_u} \mathbf{u}$ , can be used in combination with the attitude controller derived next.



3) *Attitude control*: Attitude control, as we define it here, is in charge of making the aircraft heading direction  $\mathbf{h}$  converge to the desired one  $\mathbf{h}^*$  and of ensuring a balanced flight, i.e. of zeroing the side-slip angle by zeroing the lateral velocity component  $v_{a,2} = \mathbf{v}_a \cdot \mathbf{j}$ . We show next that these two objectives can be achieved via the determination of a desired mobile frame  $\bar{\mathcal{B}} := \{G; \bar{\mathbf{i}}, \bar{\mathbf{j}}, \bar{\mathbf{k}}\}$  and the convergence of the aircraft frame  $\mathcal{B} = \{G; \mathbf{i}, \mathbf{j}, \mathbf{k}\}$  to this desired frame. We assume in this section that  $|\mathbf{v}_a|$  is always larger than some positive number and that thrust control is used to stabilise  $|\mathbf{v}|$  at the desired speed  $v^*$ .

Let us first define the desired unit vector  $\bar{\mathbf{i}}$ . From relation (16) one deduces that

$$\mathbf{z} = \frac{\mathbf{a} - \bar{\mathbf{g}} - v_{a,2} \bar{O}(\mathbf{v}_a)}{|\mathbf{a} - \bar{\mathbf{g}} - v_{a,2} \bar{O}(\mathbf{v}_a)|} \quad (25)$$

Let  $\omega_h$  denote the angular velocity of  $\mathbf{h}$ , i.e.  $\omega_h = \mathbf{h} \times \dot{\mathbf{h}}$ , and  $\bar{\omega}_h$  denote a "desired" angular velocity for the heading vector  $\mathbf{h}$  that exponentially stabilises  $\mathbf{h} - \mathbf{h}^* = 0$  when  $\omega_h = \bar{\omega}_h$ . Take, for instance

$$\bar{\omega}_h := \omega_{h^*} + k_h \tilde{\mathbf{h}} \quad (26)$$

with  $\omega_{h^*} := \mathbf{h}^* \times \dot{\mathbf{h}}^*$  denoting the angular velocity of  $\mathbf{h}^*$ ,  $\tilde{\mathbf{h}} := \mathbf{h} \times \mathbf{h}^*$ , and  $k_h$  a positive gain (not necessarily constant) whose value determines the rate of convergence of  $\mathbf{h}$  to  $\mathbf{h}^*$ . The (almost global) exponential stability of  $\mathbf{h} - \mathbf{h}^* = 0$  when  $\omega_h = \bar{\omega}_h$  then results from that  $\frac{d}{dt}(1 - \mathbf{h} \cdot \mathbf{h}^*) = -k_h |\tilde{\mathbf{h}}|^2 \leq 0$ .

A more complete solution involves a complementary integral action in charge of compensating for stationary effects of errors in the modelling of the aircraft dynamics that could prevent the convergence of  $\mathbf{h}$  to  $\mathbf{h}^*$ . Define  $\tilde{\mathbf{h}}_{\mathcal{F}}$  as the vector of coordinates of  $\tilde{\mathbf{h}}$  in the moving frame  $\mathcal{F}$ , i.e.  $\tilde{\mathbf{h}}_{\mathcal{F}} = [\mathbf{u} \cdot \tilde{\mathbf{h}}, \bar{\mathbf{u}} \cdot \tilde{\mathbf{h}}, \bar{\bar{\mathbf{u}}} \cdot \tilde{\mathbf{h}}]^\top$ . Without a complementary integral action, in the absence of wind, and along simple desired paths corresponding to classical *trim* trajectories (straight lines, horizontal circles,...), this vector would typically converge to a constant vector. To compensate for this type of bias, let  $z$  denote the (bounded) integral of  $\tilde{\mathbf{h}}_{\mathcal{F}}$  that we propose to calculate as follows

$$\begin{aligned} \dot{z} &= k_z (-z + s \bar{a} t^{\Delta_z} (z + \tilde{\mathbf{h}}_{\mathcal{F}}/k_z)) \\ z(0) &= 0_{3 \times 1} \end{aligned} \quad (27)$$

with  $\Delta_z > 0$  the chosen upperbound for  $|z(t)|$  and  $k_z$  denoting a typically large positive number. Note that  $z$  is the integral of the error  $\tilde{\mathbf{h}}_{\mathcal{F}}$  as long as  $|z|$  does not reach the saturation value  $\Delta_z > 0$ . A desired angular velocity for  $\mathbf{h}$  is then

$$\bar{\omega}_h := \omega_{h^*} + k_{h,1} \tilde{\mathbf{h}} + k_{h,2} \alpha_1(\mathbf{h}, \mathbf{h}^*, z) \mathbf{z}_{\mathcal{F}} \quad (28)$$

with  $\mathbf{z}_{\mathcal{F}} := z_1 \mathbf{u} + z_2 \bar{\mathbf{u}} + z_3 \bar{\bar{\mathbf{u}}}$ ,  $k_{h,1}$  a positive gain (not necessarily constant),  $k_{h,2} \geq 0$  a constant gain, and

$$\alpha_1(\mathbf{h}, \mathbf{h}^*, z) := \alpha^{\Delta_z} (|z + \tilde{\mathbf{h}}_{\mathcal{F}}/k_z|) \in (0, 1]$$

**Proposition 2** If  $\omega_h = \bar{\omega}_h$  with  $\bar{\omega}_h$  given by (27)-(28) then the equilibrium  $(\mathbf{h}, z) = (\mathbf{h}^*, 0_{3 \times 1})$  is almost globally asymptotically (locally exponentially) stable.

**Proof:** Define  $\mathbf{I}_h := \alpha_1(\mathbf{h}, \mathbf{h}^*, z) \mathbf{z}_{\mathcal{F}}$  so that, in view of (28)

$$\omega_h = \omega_{h^*} + k_{h,1} \tilde{\mathbf{h}} + k_{h,2} \mathbf{I}_h$$

Forming the time-derivative of  $(1 - \mathbf{h} \cdot \mathbf{h}^*)$  yields

$$\begin{aligned} \frac{d}{dt}(1 - \mathbf{h} \cdot \mathbf{h}^*) &= -\dot{\mathbf{h}} \cdot \mathbf{h}^* - \mathbf{h} \cdot \dot{\mathbf{h}}^* \\ &= -(\omega_h \times \mathbf{h}) \cdot \mathbf{h}^* - \mathbf{h} \cdot (\omega_{h^*} \times \mathbf{h}^*) \\ &= -(\omega_h - \omega_{h^*}) \cdot \tilde{\mathbf{h}} \\ &= -(\omega_h - \omega_{h^*} - k_{h,2} \mathbf{I}_h) \cdot \tilde{\mathbf{h}} \\ &\quad - k_{h,2} \mathbf{I}_h \cdot \tilde{\mathbf{h}} \\ &= -k_{h,1} |\tilde{\mathbf{h}}|^2 - k_{h,2} \mathbf{I}_h \cdot \tilde{\mathbf{h}} \end{aligned}$$

Note that

$$\mathbf{I}_h \cdot \tilde{\mathbf{h}} = \alpha_1(\mathbf{h}, \mathbf{h}^*, z) (z \cdot \tilde{\mathbf{h}}_{\mathcal{F}})$$

and also that (27) may be written as

$$\dot{z} = k_z (-z + \alpha_1(\mathbf{h}, \mathbf{h}^*, z) (z + \tilde{\mathbf{h}}_{\mathcal{F}}/k_z))$$

Therefore

$$\begin{aligned} 0.5 \frac{d}{dt} |z|^2 &= -k_z (1 - \alpha_1) |z|^2 + \alpha_1 (z \cdot \tilde{\mathbf{h}}_{\mathcal{F}}) \\ &= -k_z (1 - \alpha_1) |z|^2 + \mathbf{I}_h \cdot \tilde{\mathbf{h}} \end{aligned}$$

with the arguments of the scalar function  $\alpha_1$  omitted for the sake of legibility. Therefore, by forming the time-derivative of the positive function  $V := (1 - \mathbf{h} \cdot \mathbf{h}^*) + 0.5 k_{h,2} |z|^2$  one obtains

$$\dot{V} = -k_{h,1} |\tilde{\mathbf{h}}|^2 - 2k_{h,2} k_z (1 - \alpha_1) |z|^2 (\leq 0)$$

This latter relation yields the convergence of  $|\tilde{\mathbf{h}}|$  and  $|z|$  to zero. The exponential stability of the equilibrium  $(\mathbf{h}, z) = (\mathbf{h}^*, 0_{3 \times 1})$  then follows from the existence (easily verified) of a positive number  $c$  such that  $\dot{V} \leq -cV$  when  $|\tilde{\mathbf{h}}|$  and  $|z|$  are close to zero.

**(end of proof).**

Let us then define the "desired" acceleration

$$\mathbf{a}^* := \dot{v}^* \mathbf{h} + |v| (\bar{\omega}_h \times \mathbf{h}) \quad (29)$$

that we in turn use to define  $\bar{\mathbf{i}}$  as follows

$$\bar{\mathbf{i}} := \frac{\mathbf{a}^* - \bar{\mathbf{g}}}{|\mathbf{a}^* - \bar{\mathbf{g}}|} \quad (30)$$

For the vector  $\bar{\mathbf{j}}$  we set

$$\bar{\mathbf{j}} := \frac{\mathbf{v}_a \times \bar{\mathbf{i}}}{|\mathbf{v}_a \times \bar{\mathbf{i}}|} = \frac{\mathbf{v}_a \times (\mathbf{a}^* - \bar{\mathbf{g}})}{|\mathbf{v}_a \times (\mathbf{a}^* - \bar{\mathbf{g}})|} \quad (31)$$

and the third vector  $\bar{\mathbf{k}}$  is just calculated as the cross product of  $\bar{\mathbf{i}}$  and  $\bar{\mathbf{j}}$ , i.e.

$$\bar{\mathbf{k}} := \bar{\mathbf{i}} \times \bar{\mathbf{j}} \quad (32)$$

The above relations point out that the frame  $\bar{\mathcal{B}}$  is well defined as long as  $|\mathbf{a}^* - \bar{\mathbf{g}}|$  and  $\mathbf{v}_a \times \bar{\mathbf{i}}$  are different from zero. An important property is that, like  $\bar{\mathbf{p}}, \mathbf{v}, \mathbf{v}_a, \mathbf{g}, \omega_{h^*}$  and  $\omega_h$ , the unit vectors  $(\bar{\mathbf{i}}, \bar{\mathbf{j}}, \bar{\mathbf{k}})$  so defined do not depend on the aircraft attitude. Therefore, their time-derivatives do not depend on the aircraft angular velocity  $\omega$ . Let  $\omega_{\bar{\mathbf{i}}} := \bar{\mathbf{i}} \times \dot{\bar{\mathbf{i}}}$  and  $\omega_{\bar{\mathbf{j}}} :=$

$\bar{\mathbf{j}} \times \dot{\bar{\mathbf{j}}}$  denote the angular velocities of  $\bar{\mathbf{i}}$  and  $\bar{\mathbf{j}}$  respectively. The angular velocity of the frame  $\bar{\mathcal{B}}$  is then given by  $\bar{\boldsymbol{\omega}} = \boldsymbol{\omega}_{\bar{\mathbf{i}}} + (\bar{\mathbf{i}} \cdot \boldsymbol{\omega}_{\bar{\mathbf{j}}})\bar{\mathbf{i}} = \boldsymbol{\omega}_{\bar{\mathbf{j}}} + (\bar{\mathbf{j}} \cdot \boldsymbol{\omega}_{\bar{\mathbf{i}}})\bar{\mathbf{j}}$ , and this vector does not depend on  $\boldsymbol{\omega}$  either. The problem of stabilising  $\bar{\mathcal{B}} = \mathcal{B}$  is thus well-posed.

**Proposition 3** *Assuming that the frame  $\bar{\mathcal{B}}$  and its angular velocity  $\bar{\boldsymbol{\omega}}$  are well-defined, an angular velocity control that almost globally asymptotically (locally exponentially) stabilises  $\bar{\mathcal{B}} = \mathcal{B}$  is*

$$\boldsymbol{\omega} = \bar{\boldsymbol{\omega}} + k_{\omega}(t)((\boldsymbol{\nu} \times \bar{\mathbf{i}}) + (\mathbf{j} \times \bar{\mathbf{j}}) + (\mathbf{k} \times \bar{\mathbf{k}})) \quad (33)$$

with  $k_{\omega}(t) > \epsilon > 0$ .

This is a known result. Let us just mention, for the sake of completeness, that the proof involves the candidate Lyapunov function  $V = 0.5 \tan^2(\frac{\theta}{2})$ , with  $|\theta|$  denoting the angle between the frames  $\mathcal{B}$  at  $\bar{\mathcal{B}}$ , whose time-derivative is found equal to  $\dot{V} = -2k_{\omega}(t)V (\leq 0)$  when applying the control (33).

**Proposition 4** *If some conditions (specified and discussed next) are satisfied, then the attitude angular velocity control (33), combined with the thrust control (18)-(20), ensures the exponential convergence of the side-slip angle to zero and of  $\mathbf{h}$  to  $\mathbf{h}^*$ .*

**Proof:** By definition of  $\bar{\mathbf{j}}$ :  $v_a \cdot \bar{\mathbf{j}} = 0$ . Therefore  $v_{a,2} = v_a \cdot \mathbf{j} = v_a \cdot (\mathbf{j} - \bar{\mathbf{j}})$ . The exponential convergence of  $\mathbf{j}$  to  $\bar{\mathbf{j}}$  thus yields the exponential convergence of  $v_{a,2}$  (and of the side-slip angle) to zero. This also means that the objective of balanced flight is achieved with the angular velocity control (33). Now, since  $v_{a,2}$  exponentially converges to zero and  $\boldsymbol{\nu}$  exponentially converges to  $\bar{\mathbf{i}}$ , one deduces from relations (25) and (30) that  $\xi := \frac{\mathbf{a} - \bar{\mathbf{g}}}{|\mathbf{a} - \bar{\mathbf{g}}|} - \frac{\mathbf{a}^* - \bar{\mathbf{g}}}{|\mathbf{a}^* - \bar{\mathbf{g}}|}$  exponentially converges to zero (provided, of course, that  $|\mathbf{a} - \bar{\mathbf{g}}|$  is always larger than some positive number). In the section devoted to thrust control we have also shown that the exponential convergence of  $v_{a,2}$  to zero entailed the convergence of  $|v| - v^*$ , and subsequently of  $\frac{d}{dt}|v| - \dot{v}^*$ , to zero when an adequate thrust control, like (18)-(20), is applied. Since  $\mathbf{a} - \mathbf{a}^* = (\frac{d}{dt}|v| - \dot{v}^*)\mathbf{h} + |v|(\mathbf{h} - \bar{\boldsymbol{\omega}}_h \times \mathbf{h})$  one deduces that  $(\mathbf{a} - \mathbf{a}^*) \cdot \mathbf{h}$  exponentially converges to zero. This latter property combined with the exponential convergence of  $\xi$  to zero in turn implies that  $((\mathbf{a} - \bar{\mathbf{g}}) \cdot \mathbf{h})(\frac{1}{|\mathbf{a} - \bar{\mathbf{g}}|} - \frac{1}{|\mathbf{a}^* - \bar{\mathbf{g}}|})$  converges exponentially to zero. Therefore, provided that  $|(\mathbf{a} - \bar{\mathbf{g}}) \cdot \mathbf{h}|$  is always larger than some positive number,  $(|\mathbf{a} - \bar{\mathbf{g}}| - |\mathbf{a}^* - \bar{\mathbf{g}}|)$  converges exponentially to zero, and so does  $(\mathbf{a} - \mathbf{a}^*) \cdot \mathbf{h}$ . Therefore  $(\mathbf{h} - \bar{\boldsymbol{\omega}}_h \times \mathbf{h})$  also converges to zero exponentially. Since  $\boldsymbol{\omega}_h := \mathbf{h} \times \dot{\mathbf{h}}$  and  $\boldsymbol{\omega}_h \cdot \mathbf{h} = 0$  one then infers that  $\boldsymbol{\omega}_h$  converges exponentially to  $\bar{\boldsymbol{\omega}}_h$  and, by a minor extension of Proposition 4, that  $\mathbf{h}$  converges exponentially to  $\mathbf{h}^*$ .

**(end of proof).**

The conditions evoked in Proposition 4 are that  $|\mathbf{a} - \bar{\mathbf{g}}|$ ,  $|\mathbf{a}^* - \bar{\mathbf{g}}|$ ,  $|\mathbf{v}_a \times \bar{\mathbf{i}}|$ ,  $|\mathbf{v}_a \cdot \bar{\mathbf{i}}|$ , and  $|\mathbf{h} \cdot (\mathbf{a} - \bar{\mathbf{g}})|$  must always be larger than some positive number. The vector  $\mathbf{u}$  must

also be uniquely defined and its time-derivative  $\dot{\mathbf{u}}$  must be bounded to ensure that  $\dot{\mathbf{h}}^*$  and  $\boldsymbol{\omega}_{h^*}$  are themselves well-defined and bounded. In view of the guidance stability result of Proposition 1 and of the attitude control stability result of Proposition 3 one can also conclude that, under the same conditions, the angular velocity (33) ensures the convergence of the (modelled) aircraft to the desired path, with the desired direction. The conditions evoked previously may seem restrictive at first glance, but they are in fact inherent to the control problem at hand. They are also related to the existence of particular trajectories along which the linearised equations of the Newton equation (5) complemented with the model (8) of aerodynamic forces are not controllable. Although they are not satisfied in only very specific situations, they nonetheless rule out the possibility of global stability results. However, it remains possible to state local stability results when these conditions are satisfied on the desired path. For instance, in the case of zero wind velocity, and when  $|v| = v^*$  is constant, one verifies that the first five conditions are satisfied on the desired path if  $|\mathbf{u} \times \boldsymbol{\nu}|$  and  $|\mathbf{u} \cdot \boldsymbol{\nu}|$  are positive (and larger than a small number) on the path. Since, for a balanced flight,  $\boldsymbol{\nu} = \frac{\mathbf{a} - \bar{\mathbf{g}}}{|\mathbf{a} - \bar{\mathbf{g}}|}$  with  $\mathbf{a} = v^{*2}(\gamma_1 \bar{\mathbf{u}} + \gamma_2 \bar{\mathbf{u}})$  and  $\bar{\mathbf{g}} = \mathbf{g} - \frac{c_0}{m} v^{*2} \mathbf{u}$ , these conditions are themselves satisfied if

$$\mathbf{A1}: |\mathbf{g} \times \mathbf{u} - v^{*2}(\gamma_1 \bar{\mathbf{u}} - \gamma_2 \bar{\mathbf{u}})| > \epsilon_1 > 0 \quad (34)$$

and

$$\mathbf{A2}: |\frac{c_0}{m} v^{*2} - \mathbf{g} \cdot \mathbf{u}| > \epsilon_2 > 0 \quad (35)$$

As for the conditions concerning the boundedness of  $|\dot{\mathbf{u}}|$  and of  $|\boldsymbol{\omega}_{h^*}|$  they are satisfied if

$$\mathbf{A3}: |\gamma_1| \text{ and } |\gamma_2| \text{ are bounded, and } 1 - \gamma_1 y_1 - \gamma_2 y_2 > \epsilon_3 > 0 \quad (36)$$

The satisfaction of latter condition also ensures the uniqueness of the projection of the aircraft position on the path. We can then state the following local stability result

**Proposition 5** *Consider the Newton equation (5) complemented with the model (8) of aerodynamic forces. In the case of zero wind velocity and  $v^*$  constant ( $\neq 0$ ), if the assumptions A1-A3 are satisfied and  $\mathbf{h}^*$  is a desired heading vector that verifies the properties of Proposition 1 then the control inputs  $(T, \boldsymbol{\omega})$  given by (18)-(20) and (33) locally exponentially stabilise  $(\tilde{\mathbf{p}}_{\mathcal{F}}, \tilde{\mathbf{p}}_{\mathcal{F}}, z, \bar{\mathcal{B}}, v) = (\mathbf{0}, \mathbf{0}, 0_{3 \times 1}, \bar{\mathcal{B}}, \text{sign}_{v_u} v^* \mathbf{u})$ .*

*C. Application to particular curves*

1) *Straight line:*  $\mathcal{C}$  is a straight line passing through the point  $\mathbf{p}_c$  and with (constant) unit direction vector  $\mathbf{u}$ . Then  $\gamma_1 = \gamma_2 = 0$  so that Assumption A3 in Proposition 5 is verified. Assumption A1 is also verified provided that the path is not vertical, i.e. not parallel to the gravitational acceleration. As for Assumption A2, it gives a condition relating the desired speed to the path slope. More precisely it is verified when  $v^{*2} \neq \frac{mg_0}{c_0} \sin(\nu)$ , with  $\nu$  denoting the so-called path angle, i.e. the angle between the path and the horizontal plane. Moreover, the point  $Q$  is always unique and



its position can be directly calculated from the aircraft position  $\mathbf{p}$  and the curve characteristics  $(\mathbf{p}_c, \mathbf{u})$ . More precisely,  $\mathbf{q} = \mathbf{p}_c + (\mathbf{u} \cdot (\mathbf{p} - \mathbf{p}_c))\mathbf{u}$ ,  $\tilde{\mathbf{p}} = \mathbf{u} \times ((\mathbf{p} - \mathbf{p}_c) \times \mathbf{u})$  and any pair  $(\bar{\mathbf{u}}, \bar{\bar{\mathbf{u}}})$  of constant orthonormal vectors perpendicular to  $\mathbf{u}$  can be used for the control calculations.

2) *Circle*:  $\mathcal{C}$  is a circle centered at  $\mathbf{p}_c$  with radius  $r$  and (constant) unit vector  $\bar{\mathbf{u}}$  orthogonal to the circle's plane. Note that this plane does not have to be horizontal. Then  $\gamma_1 = \frac{1}{r}$ ,  $\gamma_2 = 0$ . Alike the straight line case, the point  $Q$  on the curve and the unit vectors  $(\bar{\mathbf{u}}, \mathbf{u})$  associated with the parallel transport frame (that coincides in this particular case with the Frénet frame) can be directly calculated from the aircraft position  $\mathbf{p}$  and the curve characteristics  $(\mathbf{p}_c, r, \bar{\mathbf{u}})$ . More precisely,  $\bar{\mathbf{u}} = \frac{((\mathbf{p} - \mathbf{p}_c) \times \bar{\mathbf{u}}) \times \bar{\mathbf{u}}}{|((\mathbf{p} - \mathbf{p}_c) \times \bar{\mathbf{u}}) \times \bar{\mathbf{u}}|}$ ,  $\mathbf{u} = \bar{\mathbf{u}} \times \bar{\bar{\mathbf{u}}}$ ,  $\mathbf{q} = \mathbf{p}_c - r\bar{\mathbf{u}}$ ,

and  $\tilde{\mathbf{p}} = \mathbf{p} - \mathbf{q}$ . One also verifies that  $\boldsymbol{\eta} = \frac{(\mathbf{u} \cdot \mathbf{v})^2}{(\mathbf{p} - \mathbf{p}_c) \cdot \bar{\mathbf{u}}} \bar{\mathbf{u}}$ .

In this case Assumption A3 becomes  $-\frac{1}{r}((\mathbf{p} - \mathbf{p}_c) \cdot \bar{\mathbf{u}}) > \epsilon_3 > 0$ , and it is not satisfied only when the aircraft is located on the circle's axis, which corresponds to the case where the aircraft is equidistant to all points on the circle (loss of uniqueness of the closest point). Assumption A1 is always verified, except in the particular case when the circle is vertical and  $g_0 = \frac{v^{*2}}{r}$ . As for Assumption A2, it is verified when  $v^{*2} > \frac{mg_0}{\bar{c}_0} \sin(\nu)$ , with  $\nu$  denoting the angle between the circle's plane and the horizontal plane.

#### IV. COMPLEMENTARY ISSUES

##### A. Extension to a curve defined on a translating frame

An extension of the path following problem addressed previously consists in considering a curve that is fixed w.r.t. a translating frame whose origin  $\mathbf{p}_c$  moves with velocity  $\mathbf{v}_c$ , i.e.  $\frac{d}{dt}\mathbf{p}_c = \mathbf{v}_c$ , and acceleration  $\mathbf{a}_c$ , i.e.  $\frac{d}{dt}\mathbf{v}_c = \mathbf{a}_c$ . For the sake of simplification we assume here that this frame does not rotate, but the extension to a rotating frame is also possible. A practical application would, for instance, consist in having an aircraft fly in circles over a moving ground target. This problem is also referred to as Moving Path Following (MPF) in [20] [19]. We leave the interested reader to verify that this extension just involves the modification of equations (10), (11), (13) and (14) according to

$$\dot{\tilde{\mathbf{p}}} = \frac{d}{dt}\vec{OG} - \frac{d}{dt}\vec{OC} - \frac{d}{dt}\vec{CQ} = (\mathbf{v} - \mathbf{v}_c) - \dot{s}\mathbf{u} \quad (37)$$

$$\begin{aligned} \dot{\tilde{\mathbf{p}}}_{\mathcal{F}} &= ((\mathbf{v} - \mathbf{v}_c) \cdot \bar{\mathbf{u}})\bar{\mathbf{u}} + ((\mathbf{v} - \mathbf{v}_c) \cdot \bar{\bar{\mathbf{u}}})\bar{\bar{\mathbf{u}}} \\ &= \Pi_{\mathbf{u}}(\mathbf{v} - \mathbf{v}_c) \end{aligned} \quad (38)$$

$$\dot{s} = \frac{((\mathbf{v} - \mathbf{v}_c) \cdot \mathbf{u})}{1 - \gamma_1 y_1 - \gamma_2 y_2} \quad (39)$$

$$\begin{aligned} \ddot{\tilde{\mathbf{p}}}_{\mathcal{F}} &= \Pi_{\mathbf{u}}\mathbf{a} + \boldsymbol{\eta} \\ \boldsymbol{\eta} &= -\Pi_{\mathbf{u}}\mathbf{a}_c - ((\mathbf{v} - \mathbf{v}_c) \cdot \mathbf{u})\dot{s}(\gamma_1 \bar{\mathbf{u}} + \gamma_2 \bar{\bar{\mathbf{u}}}) \end{aligned} \quad (40)$$

The desired heading direction  $\mathbf{h}_c^*$  ( $= \frac{\mathbf{v}}{|\mathbf{v}|}$ ) must satisfy the equation

$$\frac{\mathbf{v} - \mathbf{v}_c}{|\mathbf{v} - \mathbf{v}_c|} = \mathbf{h}^* \left( = \frac{\mathbf{h}_c^* - \frac{\mathbf{v}_c}{|\mathbf{v}|}}{|\mathbf{h}_c^* - \frac{\mathbf{v}_c}{|\mathbf{v}|}|} \right)$$

with  $\mathbf{h}^*$  given by (23). One verifies that the solution to this equation is

$$\mathbf{h}_c^* = \Pi_{\mathbf{h}^*}\mathbf{v}_c/|\mathbf{v}| + \sqrt{1 - |\Pi_{\mathbf{h}^*}\mathbf{v}_c|^2/|\mathbf{v}|^2}\mathbf{h}^* \quad (41)$$

with  $\Pi_{\mathbf{h}^*}$  denoting the operator of projection on the plane orthogonal to  $\mathbf{h}^*$ . For this desired direction to be well defined it suffices that  $|\mathbf{v}| > |\mathbf{v}_c|$ . As expected,  $\mathbf{h}_c^* = \mathbf{h}^*$  when  $\mathbf{v}_c = 0$ .

##### B. Adaptation to two-axis autopilots

The three-axis (pitch-roll-yaw) control system proposed so far does not specifically rely on the existence of a stabilising tail equipped with pitch and yaw control surfaces. All that matters is the possibility of modifying the aircraft attitude at will, like multirotor drones that use differential blade rotation to this purpose. By contrast, two-axis (either pitch-roll or pitch-yaw) control systems rely on the existence of a stabilising tail that compensates, via passive control and torque coupling, for the lack of an active control torque about one of the aircraft rotation axes. Typically tail vertical and horizontal surfaces serve to stabilise the aircraft heading along the air-velocity direction by creating passive torques that are opposed to angular variations w.r.t. the air-velocity direction.

1) *Pitch-roll control*: In particular, provided that an adequate roll angle is created, the tail vertical surface is very efficient at maintaining the side-slip angle small. This explains why active yaw control (often termed as yaw damping in relation to the comfort it brings to passengers by allowing for precise side-slip angle zeroing) via the use of a rotating rudder surface is of secondary importance for most common airplanes. This also explains the common use of two-axis pitch-roll autopilots that control airplanes automatically. With respect to the three-axis desired angular velocity  $\boldsymbol{\omega}^*$  given by (33) it thus essentially suffices to create, via elevator and ailerons actions, pitch and roll torques that asymptotically stabilise  $\omega_1 - \omega_1^*$  and  $\omega_2 - \omega_2^*$  at zero. This can be achieved without creating a yaw torque with the tail rudder.

2) *Pitch-Yaw control*: This type of two-axis attitude control, involving tail elevator and rudder action only, is more involved due to the absence of wing ailerons that directly produce the desired roll torque. In this case roll is indirectly, and less efficiently, produced by yaw via the action of the tail rudder in combination with the existence of a main-wing dihedral and/or a main wing located significantly above the aircraft CoM. This configuration also requires the existence of a tail vertical surface that creates yaw stabilisation and resistance to slideslip.

To be more specific, and give some insight of a possible yaw-roll control solution, let us consider the case of an airplane with a (small) dihedral angle  $\theta$ . By applying the model (8) of aerodynamic forces to both sides of the main wing with  $c_0 \ll \bar{c}_0$  one shows that the aerodynamic roll torque is approximately given by

$$\boldsymbol{\Gamma}_{a,roll} \approx l\bar{c}_0 \left( -(\theta v_{a,2} + l\omega_1)v_{a,1} + lv_{a,3}\omega_3 \right) \mathbf{z}$$

with  $l$  denoting the lateral distance between the aircraft CoM and the points of application, on both sides of the wing, of resultant aerodynamic forces. In the absence of actuated ailerons this is the main roll torque acting on the aircraft, and the Euler equation thus becomes in the first approximation

$$J\dot{\omega} \approx -S(\omega)J\omega + \begin{pmatrix} \Gamma_{a,roll} \\ \Gamma_{2,3} \end{pmatrix}$$

with  $\Gamma_{2,3}$  the vector of directly controlled pitch and yaw torques. Assuming that  $J = \text{diag}\{j_1, j_2, j_3\}$  with  $j_2 \approx j_3$ , the first line of this vectorial equation, combined with the expression of  $\Gamma_{a,roll}$ , yields

$$\dot{\omega}_1 \approx \frac{l\bar{c}_0}{j_1} \left( -(\theta v_{a,2} + l\omega_1)v_{a,1} + lv_{a,3}\omega_3 \right) \quad (42)$$

This relation already indicates that a balanced flight (i.e. with  $v_{a,2} = 0$ ) is no longer possible when the aircraft turns. Indeed, consider for instance the case of a horizontal circular trajectory followed with a constant speed and a constant roll angle, i.e. such that  $\omega_1 = \dot{\omega}_1 = 0$  and  $\omega_3$  is constant. Then (42) yields  $v_{a,2} \approx \frac{l\alpha}{\theta}\omega_3$ , with  $\alpha = v_{a,3}/v_{a,1}$  approximately equal to the attack angle. This relation also indicates that  $v_{a,2}$  is inversely proportional to the dihedral angle  $\theta$ .

Another relation of interest concerns the dependence of  $v_{a,2}$  upon the other velocity components. In the model (8) of aerodynamic forces, setting  $v_{a,2}\mathbf{O}(v_a) \approx -\bar{c}_0 v_{a,2}|v_a|\mathbf{j}$ , with  $\bar{c}_0 > 0$  denoting the coefficient of resistance to lateral motion, and using this model in the Newton equation (5), yields

$$\dot{v}_2 \approx -\omega_3 v_1 + \omega_1 v_3 + g_2 - \frac{\bar{c}_0}{m} v_{a,2}|v_a|$$

with  $g_2 = \mathbf{g} \cdot \mathbf{j}$ . By neglecting the wind velocity and using  $|v_a| \approx v_{a,1}$  this relation becomes

$$\dot{v}_{a,2} \approx -\omega_3 v_{a,1} + \omega_1 v_{a,3} + g_2 - \frac{\bar{c}_0}{m} v_{a,1} v_{a,2}$$

A large resistance coefficient  $\bar{c}_0$ , whose value essentially depends on the aircraft body profile and the size of the vertical stabiliser, in turn implies that

$$v_{a,2} \approx \frac{m}{\bar{c}_0} \left( -\omega_3 + \frac{v_{a,3}}{v_{a,1}} \omega_1 + \frac{g_2}{v_{a,1}} \right)$$

Using this relation in (42) then yields

$$\dot{\omega}_1 \approx \frac{l\bar{c}_0}{j_1} \left( -\left( \frac{m\theta}{\bar{c}_0} v_{a,3} + lv_{a,1} \right) \omega_1 + \left( \frac{m\theta}{\bar{c}_0} v_{a,1} + lv_{a,3} \right) \omega_3 - \frac{m\theta}{\bar{c}_0} g_2 \right)$$

and, using the fact that the attack angle ( $\approx v_{a,3}/v_{a,1}$ ) is nominally very small

$$\dot{\omega}_1 \approx \frac{l^2 \bar{c}_0 v_{a,1}}{j_1} \left( -\omega_1 + \frac{m\theta}{\bar{c}_0 l} \left( \omega_3 - \frac{g_2}{v_{a,1}} \right) \right)$$

This latter relation illustrates the known fact that yaw authority over roll increases with the dihedral angle  $\theta$ . In view of the nominally large gain  $\frac{l^2 \bar{c}_0 v_{a,1}}{j_1}$ , if the dynamics of  $\omega_1^*$  is "enough slow" (a feature that can be enforced via filtering and saturation), the previous relation suggests to choose

$$\omega_3^* = \frac{g_2}{v_{a,1}} + k_{\omega_3} \omega_1^* \quad (k_{\omega_3} > 0) \quad (43)$$

for the desired value of  $\omega_3$ , so as to have  $\omega_1$  approximately converge to  $\frac{k_{\omega_3} m \theta}{\bar{c}_0 l} \omega_1^*$  when  $\omega_3$  converges to  $\omega_3^*$ . Accordingly, choosing  $k_{\omega_3} = \frac{\bar{c}_0 l}{m \theta}$  would make the yaw induced roll velocity  $\omega_1$  tend to the desired roll angular velocity  $\omega_1^*$ , except that this choice is only theoretical due to the imprecise knowledge of the parameters  $l$  and (more particularly)  $\bar{c}_0$ . This latter issue is fortunately not very sensitive because  $\omega_1^*$ , as given by (33), is essentially a feedback control term whose gain can be multiplied by a positive term without much affecting the control performance. From there it remains to produce (via tail rudder action) a yaw torque that stabilises  $\omega_3 - \omega_3^* = 0$  asymptotically. The complementary production of a pitch torque that stabilises  $\omega_2 - \omega_2^*$  at zero then yields a pitch-yaw control that mimics (up to some limitations) the pitch-roll control evoked previously.

### C. From desired body angular velocity to control-surfaces angles velocities

Consider a fixed-wing aircraft equipped with standard roll-pitch-yaw control surfaces. Let  $\delta = [\delta_1, \delta_2, \delta_3]^T$  denote the vector of control-surfaces angles that have to be calculated from the desired body angular velocity  $\omega^*$  determined previously. The preliminary step relies on the determination/estimation of the matrix-valued function  $A(v_a, \omega) =: \frac{\partial \Gamma}{\partial \delta} |_{\delta=0}$  that relates angles deviations to torque production for small angles. This function is aircraft specific. It depends in particular on the placement of the control surfaces with respect to the aircraft CoM and on their dimensions. Typically, along classical trim trajectories and nominal air velocities involving small attack and side-slip angles,  $A(v_a, \omega)$  can be approximated by  $|v_a|^2 \bar{A}$ , with  $\bar{A}$  a constant matrix. We assume from now on that  $A$ , or at least an estimate of this matrix-valued function, is known. Since  $J\dot{\omega} \approx -S(\omega)J\omega + \Gamma$  one deduces that a torque equal to  $\Gamma^* = S(\omega)J\omega^* - k_\gamma J(\omega - \omega^*)$ , with  $k_\gamma$  a large positive gain, is effective to make  $\omega$  track  $\omega^*$ . This in turn suggests to make  $\delta$  track  $\delta^* =: A^{-1}\Gamma^*$  by setting  $\dot{\delta} = u_\delta$  with  $u_\delta =: -k_\delta(\delta - \delta^*)$  and  $k_\delta$  a positive gain. However, control surfaces angular velocities, as well as angles, are usually bounded. Let  $\bar{u}_{\delta,i}$  ( $i = 1, 2, 3$ ) denote the saturated value of  $u_{\delta,i}$ , and  $\Delta_{\delta,i}$  the maximal value of  $\delta_i$ . A possible driving law for each control surface angle that respects these bounds is then

$$\dot{\delta}_i = -\bar{k}_\delta \delta_i + \bar{k}_\delta \text{sat}^{\Delta_{\delta,i}}(\delta_i + \bar{u}_{\delta,i}/\bar{k}_\delta), \quad i = 1, 2, 3$$

with  $\bar{k}_\delta$  denoting a large positive gain.

### D. Thrust bounds and attack angle monitoring

We have so far assumed that the aircraft could produce the desired thrust  $T$  calculated according to (18)-(20). In practice this desired value of  $T$  may leave the physical thrust interval  $[T_{min}, T_{max}]$ . When this happens at least one of the control objectives -i.e. convergence of the aircraft heading direction  $\mathbf{h}$  to the desired one  $\mathbf{h}^*$  (or  $\mathbf{h}_c^*$ ), or stabilisation of  $|v|$  at the desired speed  $v^*$ - cannot (momentarily) be achieved with the available thrust. For instance, descending from a high altitude to a horizontal circular path with the convergence dynamics specified by  $\mathbf{h}^*$  may require a negative thrust (to

slow down the aircraft) that a common aircraft, for which  $T_{min} \approx 0$ , cannot produce. Similarly, ascending with these convergence dynamics and velocity may require a thrust that exceeds  $T_{max}$ .

To avoid this situation a possibility consists in reducing the rate of convergence to the desired path in order to have the control action focused on the stabilisation of the aircraft velocity about the desired speed  $v^*$ . This can be done, for instance, by choosing the parameter  $\mu$  in the expression of the saturation  $\Delta_h := \frac{\mu|v|}{k_1 \max(d_1, d_2)}$  small enough. Provided that  $v^*$  can be maintained on the desired path with the available thrust (meaning for instance, in the case of a straight path and assuming that  $(-sign_{v_u} mg \cdot u + c_0 v^{*2}) \in [T_{min}, T_{max}]$ ), this strategy can ensure that the calculated thrust  $T$  will ultimately remain in the interval  $[T_{min}, T_{max}]$  whatever the initial position and orientation of the aircraft. In the case of a horizontal path one may alternatively set the parameter  $d_2$  small enough so as to impose a (small) rate of climb or descent, during the transient phase of convergence to the path, that is compatible with the thrust limitations.

The aforementioned possibility aims at keeping the calculated thrust within the range  $[T_{min}, T_{max}]$  so that both control objectives can simultaneously be achieved. However, one may also temporarily accept an increase of the aircraft velocity beyond the desired speed  $v^*$  during a descending transient phase when a negative thrust (needed to slow down the aircraft) is calculated and cannot be produced (i.e. when  $T_{min} = 0$ ). In this case only the objective of convergence of the heading direction  $\mathbf{h}$  to the desired one  $\mathbf{h}^*$  is maintained. This implicitly means that the current aircraft speed obtained with zero thrust (the saturated value closest to the calculated negative thrust) coincides with the desired speed, i.e.  $v^*(t) = |v(t)|$ . This in turn yields to setting  $\dot{v}^* = \frac{d}{dt}|v|$  in the relation (29) that defines the desired acceleration  $\mathbf{a}^*$ . This supposes that  $\frac{d}{dt}|v|$  is either estimated or measured. This choice can also be opted for when thrust control is used to stabilise the air-velocity component  $v_{a,1}$  instead of  $|v|$ .

A different issue concerns positive thrust limitations. Indeed, while unlimited thrust power theoretically allows one to control an aircraft at any speed and attack angle, a finite value  $T_{max}$  automatically limits the aircraft speed (even in a deep dive situation). Moreover, when the maximal thrust is significantly smaller than the aircraft weight it critically matters to keep the attack angle small (and under the stall value). Without this safety feature the direction  $\bar{\mathbf{i}}$  that is calculated (or imposed by a pilot) without taking this limitation into consideration may yield a large angle of attack and a loss of lift leading to a continuing descent (even at full thrust) and the crash of the aircraft. The Air France Airbus tragedy in 2009, between Rio de Janeiro and Paris, is a sad illustration of this. To automatically integrate this safety feature in the proposed control design let us rename the unit vectors  $\{\bar{\mathbf{i}}, \bar{\mathbf{j}}, \bar{\mathbf{k}}\}$  calculated without taking thrust limitations into account as  $\{\bar{\mathbf{i}}^*, \bar{\mathbf{j}}^*, \bar{\mathbf{k}}^*\}$ . Let also  $\alpha_{max}$  denote the desired upperbound for the attack angle. Whenever the predicted attack angle  $\alpha^* := \arcsin(\frac{v_a}{|v_a|} \cdot \bar{\mathbf{k}}^*)$  is larger than  $\alpha_{max}$  we

propose to determine new desired attitude directions for the aircraft such that the associated attack angle is equal to  $\alpha_{max}$ . More precisely, we propose to set

$$\bar{\mathbf{i}} = rot(\alpha_{max} \bar{\mathbf{j}}^*) \frac{v_a}{|v_a|}, \quad \bar{\mathbf{j}} = \bar{\mathbf{j}}^*, \quad \bar{\mathbf{k}} = \bar{\mathbf{i}} \times \bar{\mathbf{j}} \quad (44)$$

with  $rot(\alpha_{max} \bar{\mathbf{j}}^*) \frac{v_a}{|v_a|}$  denoting the vector  $\frac{v_a}{|v_a|}$  rotated by the angle  $\alpha_{max}$  about the unit vector  $\bar{\mathbf{j}}^*$ . Note that this choice corresponds to the minimization of  $|\bar{\mathbf{i}} - \bar{\mathbf{i}}^*|$  under the constraint  $\arcsin(\frac{v_a}{|v_a|} \cdot \bar{\mathbf{k}}) = \alpha_{max}$ . In other words the proposed procedure minimizes the modifications brought to the calculated desired directions under the constraint of keeping the attack angle at most equal to the chosen threshold. Note also that the new attitude directions  $\{\bar{\mathbf{i}}, \bar{\mathbf{j}}, \bar{\mathbf{k}}\}$ , alike  $\{\bar{\mathbf{i}}^*, \bar{\mathbf{j}}^*, \bar{\mathbf{k}}^*\}$ , do not depend on the aircraft orientation so that the stabilisation of these directions via the angular velocity input  $\omega$  specified in relation (33) remains a well-posed problem. In this case the pre-compensation velocity  $\bar{\omega}$  is calculated with  $\omega_{\bar{\mathbf{i}}} := \bar{\mathbf{i}} \times \dot{\bar{\mathbf{i}}}$  and, in view of (44)

$$\dot{\bar{\mathbf{i}}} = \alpha_{max} \omega_{\bar{\mathbf{j}}^*} \times \bar{\mathbf{i}} + rot(\alpha_{max} \bar{\mathbf{j}}^*) \Pi_{\frac{v_a}{|v_a|}} \frac{\dot{v}_a}{|v_a|}$$

The convergence of  $\{\mathbf{i}, \mathbf{j}, \mathbf{k}\}$  to  $\{\bar{\mathbf{i}}, \bar{\mathbf{j}}, \bar{\mathbf{k}}\}$  then ensures that the aircraft attack angle is ultimately bounded by  $\alpha_{max}$ .

When implementing this safety procedure (again imposed by a limited maximal thrust) one must further pay attention to choosing the desired speed  $v^*$  larger (with some security margin) than the horizontal speed that can be sustained when the attack angle is kept equal to  $\alpha_{max}$ . The reason is that a smaller horizontal speed calls for a larger attack angle that is no longer allowed for by the controller. Imposing such a speed will thus result in the aircraft going down.

## V. SIMULATIONS

### A. Hardware-in-the-loop

The object of this section is to test and validate via realistic simulation the path following control approach reported in the previous sections. A particularity of the proposed simulations is that they are *hardware-in-the-loop* implemented in the sense that the control algorithms are implemented on a piece of hardware that could equip a physical UAV aircraft. The only difference with a true experimentation is that this hardware is connected to a computer simulated model of an aircraft that closely mimics the dynamics of a physical aircraft. This type of simulation is widely recognized for its convenience and soundness.

1) *Aircraft simulator*: We use the *X-plane 10* software, a Laminar Research product, as a flight simulator (<http://www.x-plane.com/desktop/how-x-plane-works/>). X-plane implements an aerodynamic model based on the so-called blade element theory. This method takes into consideration the geometry of the plane and the different airfoil shapes. It decomposes the wings, horizontal and vertical stabilisers into a finite number of elements. Aerodynamic forces are then determined for each element depending on its orientation and the air-velocity at its location on the aircraft. Force calculations take downwash and propwash effects into

consideration, with finite-wing corrections applied to 2D airfoil data depending on the wings geometry. Compressible flow effects are also taken into account. This approach differs from others that traditionally calculate aerodynamic forces from stability derivatives and lookup tables, and whose precision is tied to data acquired from wind tunnels measurements and/or advanced CFD simulations. Another asset of this simulation technique, particularly interesting for scale-model UAVs, is that the obtained flight model is not limited to a small flight envelope. One can also design a custom aircraft model by using the "Plane-Maker" tool included in X-plane and create a custom airfoil force model by using the "Airfoil-Maker" tool. For the present simulations, we have used a publicly available model of a scale UAV created with the previously cited tools and based on a PT-60 RC model. Some specifications of the model are:

- Wingspan: 1.8m
- Wing surface: 0.6m<sup>2</sup>
- Fuselage length: 1.72m
- Weight: 3.6 kg

2) *Controller hardware and software:* A commercially available "Pixhawk", equipped with a 168 MHz ARM Cortex M4F CPU and 256 KB of RAM, is used as the autopilot hardware. Our code implementation is based on the open-source PX4 flight stack that runs on top of a NuttX real-time operating system and uses the PX4 middleware [15]. This software architecture runs different threads with a modular approach and handles inter-process communications, allowing for the development and use of off-the-shelf control code. We took advantage of this possibility to replace the pre-existing position and attitude control modules by our own libraries in order to implement the control algorithms presented in the paper. However we kept the other pre-existing functionalities and, in particular, the EKF state observer. Flight data is logged on a SD card, allowing for post-processing and analysis of this data.

3) *Ground control station:* We use the "Qgroundcontrol" software<sup>1</sup> as a control station installed on a base computer, to design missions and change parameters online during flights. In our simulation setup, Qgroundcontrol connects the base computer to the "PIXHAWK" controller via USB using the "MAVLINK" protocol. In parallel, Qgroundcontrol establishes a UDP link with the X-plane simulator to send and receive data. This dual connection allows Qgroundcontrol to perform hardware-in-the-loop simulation by allowing an indirect communication between the controller and the simulator. Simulated position and attitude of the aircraft are used to create virtual sensory measurements (GPS, IMU, barometer, pitot) that are purposefully corrupted with artificial noise and produced (sent) at a realistic rate. These measurements are processed by the included EKF state observer and are used to calculate PWM (Pulse-width-Modulation) control values. The controller sends these control values to the ground station, which in turn sends them to the simulator

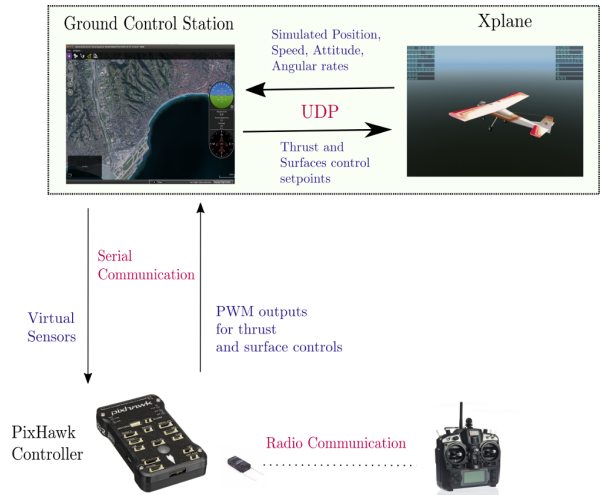


Fig. 4. HITL tools

that uses them as setpoints for the airplane's propeller angular velocity and for the control surfaces angles.

4) *Calculation of PWM control inputs:* Thrust is produced by the airplane's propeller. A relation classically used between the propeller angular velocity  $\delta_t$ , whose PWM value is encoded between 0 and 1, and the produced thrust force is  $T = k_{prop}((k_{motor}\delta_t)^2 - |v_{a,1}|^2)$ , with  $k_{prop}$  and  $k_{motor}$  denoting positive constant gains. For the simulations we have purposefully neglected the term  $|v_{a,1}|^2$  and used  $k_{prop}k_{motor}^2 = 28$ . The integral action incorporated in the thrust control law is there to compensate for this type of modelling error and our imprecise estimation of the gains  $k_{prop}$  and  $k_{motor}$ . As for the servo motors acting on the control surfaces they receive PWM setpoint signals whose encoded values  $\Delta_i$  ( $i = 1, 2, 3$ ) are comprised between  $-1$  and  $1$ . These latter values correspond to maximum deflection angles of the control surface on both sides of the neutral zero angle value. Knowing that the maximum deflection angle for the simulated airplane is about  $0.25rad$  we have used  $\delta_i = 0.25\Delta_i$  to relate the control surface angle  $\delta_i$  to the corresponding value of  $\Delta_i$ .

## B. Simulation Results

For these simulations the aircraft inertial position  $\mathbf{p}$ , velocity  $\mathbf{v}$ , attitude  $(\mathbf{i}, \mathbf{j}, \mathbf{k})$ , and angular velocity  $\boldsymbol{\omega}$  are supposed to be measured (by using on-board GPS and gyrometers, for instance) and are thus available for control computations. The air-velocity component  $v_{a,1}$ , as measured by a pitot tube along the aircraft longitudinal direction  $\mathbf{z}$ , is also available and the demanded airspeed for  $v_{a,1}$  is  $15m/s$ . For the reported simulations we have assumed that an *a priori* unknown wind may be present so that we can never presume that the air-velocity  $\mathbf{v}_a$  is equal to the aircraft inertial velocity  $\mathbf{v}$ . Besides  $v_{a,1}$  the other components of  $\mathbf{v}_a$  involved in the control expressions can be measured and/or estimated in various manners by fusing the information provided by complementary sensors. Now, it is also possible to derive and use an approximation of  $\mathbf{v}_a$  based on the

<sup>1</sup><http://qgroundcontrol.com/>

aircraft model equations (5) and (8) and on the sole direct measurement of the component  $v_{a,1}$ . Let us further elaborate on this possibility. From (16), and considering that the non-specified transversal component  $v_{a,2}\bar{O}(v_a)$  of the resultant aerodynamic force is parallel to  $\mathbf{j}$ , one gets  $\mathbf{a}\cdot\mathbf{k} = \bar{\mathbf{g}}\cdot\mathbf{k}$ . Therefore, using the expression (17) of  $\bar{\mathbf{g}}$  one deduces that  $v_{a,3} = \mathbf{v}_a\cdot\mathbf{k} = \frac{m}{\bar{c}_0|v_a|}(\mathbf{g}-\mathbf{a})\cdot\mathbf{k}$ . Approximating  $|v_a|$  by  $|v_{a,1}|$  and using an estimation  $\hat{\mathbf{a}}$  of the aircraft acceleration, an approximation of  $v_{a,3}$  is  $\hat{v}_{a,3} = \frac{m}{\bar{c}_0|v_{a,1}|}(\mathbf{g}-\hat{\mathbf{a}})\cdot\mathbf{k}$ . To estimate  $\hat{\mathbf{a}}$  one may use on-board accelerometers that measure the gravity acceleration minus the body acceleration, i.e.  $\mathbf{acc} = \mathbf{g}-\mathbf{a}$  so that  $\mathbf{a} = \mathbf{g}-\mathbf{acc}$  ( $= \hat{\mathbf{a}}$ ). Another possibility consists in estimating  $\mathbf{a}$  from the measurement of the inertial velocity  $\mathbf{v}$  obtained, for instance, with a GPS. Further assuming that  $\mathbf{v}$  is almost constant in the body frame yields the crude estimation  $\hat{\mathbf{a}} = \boldsymbol{\omega} \times \mathbf{v}$ . An even cruder estimation is obtained by assuming that the aircraft acceleration is small, i.e.  $\hat{\mathbf{a}} \simeq 0$ . Concerning the sideslip velocity component  $v_{a,2}$ , we assume that it is nominally small by virtue of the strong energy dissipation along the aircraft transversal direction that results from the existence of a tail rudder and, to a smaller extent, from the oblong shape of the body aircraft (this dissipation is actively re-enforced by the balanced flight control policy). The resulting approximation of  $\mathbf{v}_a$  is then  $\hat{\mathbf{v}}_a = v_{a,1}\mathbf{i} + \hat{v}_{a,3}\mathbf{k}$ . This solution seems convenient for scale-model UAVs that are not equipped with dedicated sensors that measure  $\mathbf{v}_a$  in all three directions. We have used it with  $\hat{\mathbf{a}} = 0$  to test the control robustness.

Besides the three-axis controller developed in the paper we have tested, for validation and comparison purposes, the two-axis (pitch-roll and pitch-yaw) adaptations proposed in Section IV-B. In the pitch-yaw control case we found it useful to increase the main wing dihedral angle from  $3^\circ$  to  $5^\circ$  in order to improve the control authority and reach a comparatively acceptable performance.

The aerodynamic coefficients used for the control calculations are:  $c_0 = 0.014$ , and  $c_1 = 0.8$ . These coefficients correspond to a glide rate equal to 5.4 and a gliding speed equal to  $15.3\text{m/s}$  (see the Appendix).

Two sets of control parameters have been used, depending on the controller's type. For the three-axis and two-axis pitch-roll controllers the parameters are:

- Guidance:  $k_1 = 1.5$ ,  $\mu = 0.5$ ,  $d_1 = 1$ ,  $d_2 = 0.4$
- Velocity/airspeed control:  $k_{T,1} = 2.5$ ,  $k_{T,2} = k_{T,1}^2/4$
- Heading stabilisation:  $k_{h,1} = 3$ ,  $k_{h,2} = 2.25$ ,  $\Delta_z = 0.3$ ,  $k_z = 10$
- Attitude control:  $k_\omega = 8.0$

For the two-axis pitch-yaw controller the parameters are:

- Guidance:  $k_1 = 0.375$ ,  $\mu = 0.5$ ,  $d_1 = 1$ ,  $d_2 = 1$
- Velocity/airspeed control:  $k_{T,1} = 2.5$ ,  $k_{T,2} = k_{T,1}^2/4$
- Heading stabilisation:  $k_{h,1} = 3$ ,  $k_{h,2} = 2.25$ ,  $\Delta_z = 0.3$ ,  $k_z = 10$
- Attitude control:  $k_\omega = 8.0$ ,  $k_{\omega_3} = 0.75$

For the saturation functions  $\bar{\text{sat}}^\Delta(x) = \alpha^\Delta(|x|)x$  entering the control laws we have implemented, in discrete time, the classical vector-valued saturation function, i.e. with

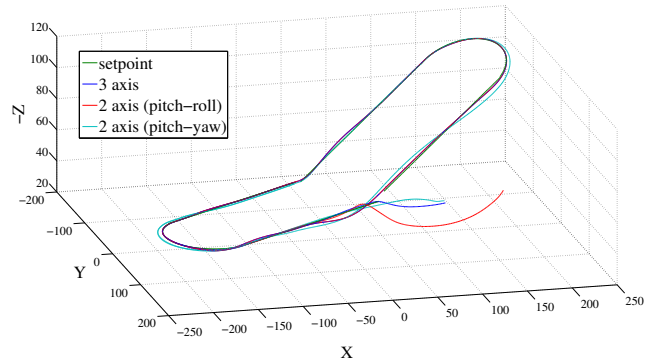


Fig. 5. Trajectory and reference path (with no wind)

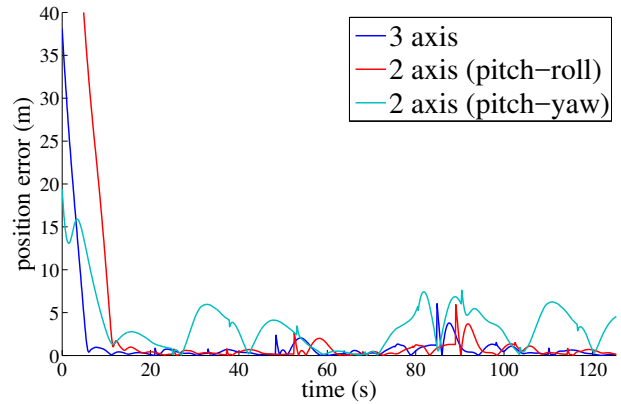


Fig. 6. Position error  $|y|$  (with no wind)

$\alpha^\Delta(|x|) = \max(1, \frac{\Delta}{|x|})$ . As explained in section IV-C, control surfaces angles are calculated according to  $\delta^* = -\frac{k_\gamma}{|v_a|^2} \bar{\mathbf{A}}^{-1} J(w-w^*) = -\frac{1}{|v_a|^2} \text{diag}([85, 100, 75])(w-w^*)$ . The term  $S(w)Jw^*$  is purposefully neglected because its contribution is not important compared to other terms. The actuators angular velocities are also limited to  $1\text{rad/s}$  by simply monitoring the difference between computed consecutive angle values.

The chosen closed reference curve (see Fig. 5) consists, for the first part, of a horizontal segment connected to a horizontal half-circle of radius equal to  $50\text{m}$ , followed by another horizontal segment. The second part of the reference path is similar to the first one except that it is inclined with an angle of  $15^\circ$  w.r.t. the horizontal plane. Just recall here that an inclined circular path does not qualify as a trim trajectory.

The first set of simulations is carried out with no wind so that one can appreciate the controllers performance in this "ideal" case. Comparative simulations results are reported in Fig. 5 and Fig. 6. They show that the three controllers allow the aircraft to approach the desired path and then follow it closely. As expected, a performance degradation is nonetheless observable in the case of the pitch-yaw controller. Despite the approximations involved in the estimation of the air-velocity  $\mathbf{v}_a$ , the imperfections of the model used for the control design, and the noisy state estimates produced by the embedded EKF observers, the other two controllers

nominally maintain the magnitude of the position error well under the accepted norm of a wingspan. Larger errors only occur when the aircraft has to switch from one piece of the curve to the next one.

Fig. 7 shows the time evolution of various variables in the case of the three-axis controller. From these figures one can pinpoint the descent phase starting at  $t \approx 70s$  and yielding the zeroing of the thrust during the time-period when the requested computed value is negative and the air-velocity component  $v_{a,1}$  exceeds the desired speed. For

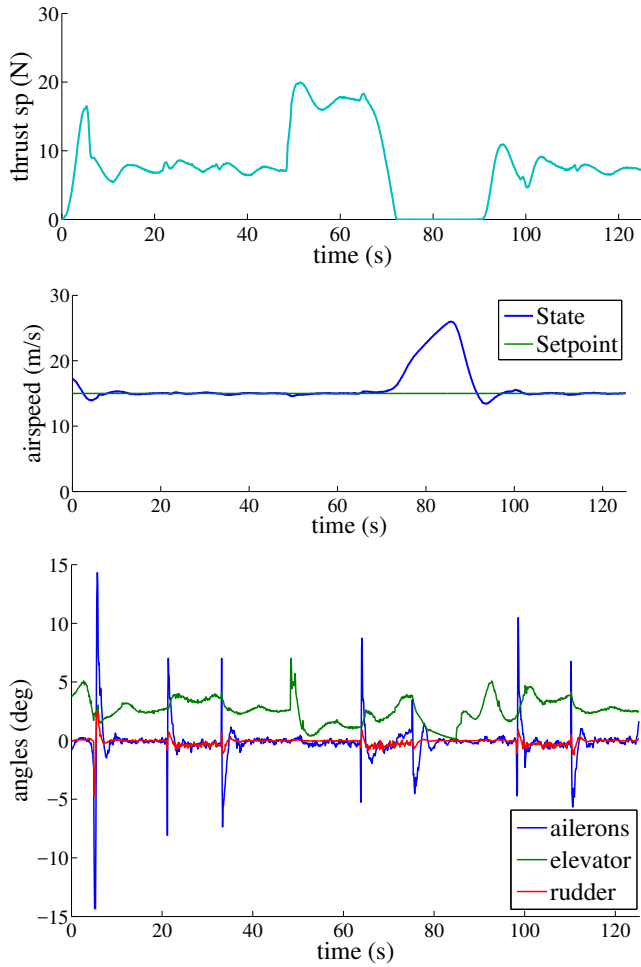


Fig. 7. 3-axis aircraft: (a) thrust setpoint (b) airspeed  $v_{a,1}$  (c) angles of control surfaces

the second set of simulations a steady (*a priori* unknown) wind of intensity  $|v_w| = 5.14m/s$  blowing from the North (corresponding to the X-axis in Fig. 5) has been added to the X-plane scenario. Despite an inevitable (mild) performance degradation, Fig. 8 and Fig. 9 show that the proposed controllers, implemented with the basic air-velocity estimator evoked previously, continue to operate properly in this case.

## VI. CONCLUDING REMARKS

The present paper provides a detailed development of a new control approach to the path following problem of scale-model airplanes. It departs from existing approaches

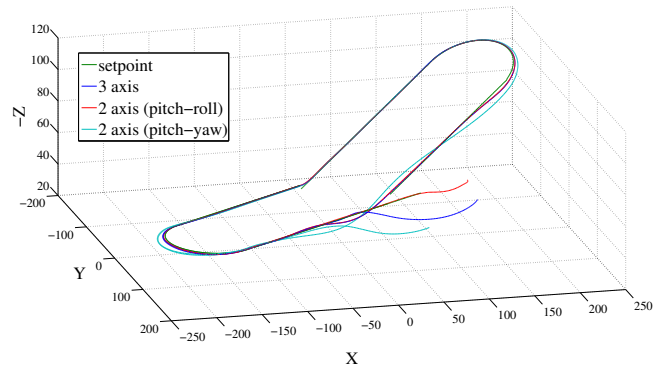


Fig. 8. Trajectory and reference path (with wind)

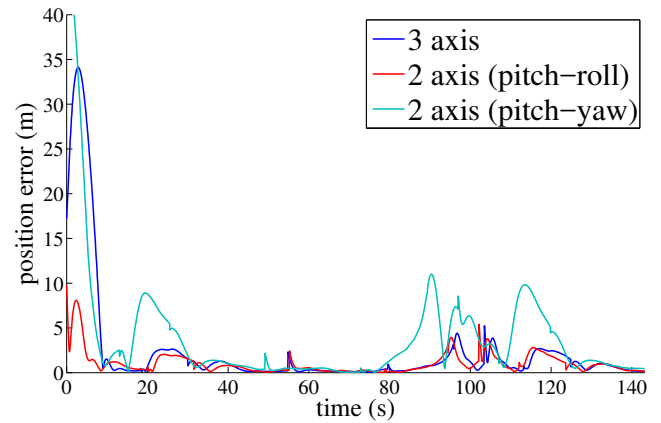


Fig. 9. Position error  $|y|$  (with wind)

by proposing a single coherent framework for kinematic guidance and dynamic control. The approach builds upon a simple analytic model of aerodynamic forces acting on the vehicle, and the resulting nonlinear controllers are designed to operate in a large spectrum of operating conditions. In particular they overcome the limitations associated with classical methods based on linearisation of aircraft dynamics equations along so-called trim trajectories. Reported realistic hardware-in-the-loop simulations illustrate the proposed control methodology, its applicability to three-axis and two-axis autopilots, and its robustness w.r.t modelling, measurements, and estimation approximations. The next logical stage of this study will involve intensive experimentation on different scale-model airplanes.

## APPENDIX: AERODYNAMIC FORCES COEFFICIENTS IN RELATION TO GLIDE RATE AND VELOCITY

The glide rate and corresponding glide velocity of an aircraft can be determined experimentally in various manners. We here recall the relations between these quantities and the coefficients  $c_0$  and  $\bar{c}_0 = c_0 + 2c_1$  used in the control design model. Comparison of experimentally measured and model-based values can in turn be used to estimate coefficients  $c_0$  and  $c_1$  yielding the best fit.

The *glide rate*  $gr$  is commonly defined as the largest possible ratio between constant horizontal and vertical speeds of the



aircraft in the vertical plane (i.e. the smallest rate of descent) when no thrust is applied. In the case of the dynamics model here considered one easily verifies that

$$gr = \frac{1 - c_0/\bar{c}_0}{2\sqrt{c_0/\bar{c}_0}}$$

In the nominal case where  $c_0/\bar{c}_0 \ll 1$  this relation simplifies to

$$gr \approx 0.5\sqrt{c_0/\bar{c}_0}$$

With the same approximation the corresponding gliding speed is given by

$$|v_{gr}| \approx \sqrt{m|g|}/(c_0\bar{c}_0)^{0.25}$$

#### REFERENCES

- [1] A. Pedro Aguiar, Joo P. Hespanha, and Petar V. Kokotovi. Performance limitations in reference tracking and path following for nonlinear systems. *Automatica*, 44(3):598 – 610, 2008.
- [2] Matthew E Argyle and Randal W Beard. Nonlinear total energy control for the longitudinal dynamics of an aircraft. In *American Control Conference (ACC), 2016*, pages 6741–6746. IEEE, 2016.
- [3] Randal W. Beard and Timothy W. McLain. *Small Unmanned Aircraft: Theory and Practice*. Princeton University Press, Princeton, NJ, USA, 2012.
- [4] Richard Bishop. There is more than one way to frame a curve. 82:Mathematical Association of America, 03 1975.
- [5] F. Le Bras, T. Hamel, R. Mahony, C. Barat, and J. Thadasack. Approach maneuvers for autonomous landing using visual servo control. *IEEE Transactions on Aerospace and Electronic Systems*, 50(2):1051–1065, April 2014.
- [6] Morten Breivik and Thor I Fossen. Principles of guidance-based path following in 2d and 3d. In *Decision and Control, 2005 and 2005 European Control Conference. CDC-ECC'05. 44th IEEE Conference on*, pages 627–634. IEEE, 2005.
- [7] L. Carter and J. Shamma. Gain-scheduled bank-to-turn autopilot design using linear parameter varying transformations. *Journal of Guidance, Control and Dynamics*, 27(5):1056–1063, 1996.
- [8] B. Escande. *Nonlinear dynamic inversion and LQ techniques*. In: Magni JF., Bennani S., Terlouw J. (eds) *Robust Flight Control*, Lecture Notes in Control and Information Sciences, vol 224. Springer, Berlin, Heidelberg, 1997.
- [9] G. Duan G. Cai and C. Hu. A velocity-based lpv modeling and control framework for airbreathing hypersonic vehicle. *International Journal of Innovative Computing, Information and Control ICIC International*, 7(5):2269–2281, 2011.
- [10] Andrew J. Hanson and Hui Ma. Parallel transport approach to curve framing. Technical report, 1995.
- [11] Minh-Duc Hua, Tarek Hamel, Pascal Morin, and Claude Samson. Introduction to feedback control of underactuated vtol vehicles: A review of basic control design ideas and principles. *IEEE Control Systems*, 33(1):61–75, 2013.
- [12] Jean-Marie Kai, Tarek Hamel, and Claude Samson. A nonlinear approach to the control of a disc-shaped aircraft. In *IEEE CDC 2017 56th IEEE Conference on Decision and Control*, 2017.
- [13] Anthony A Lambregts. Vertical flight path and speed control autopilot design using total energy principles. 1983.
- [14] Taeyoung Lee, Melvin Leoky, and N Harris McClamroch. Geometric tracking control of a quadrotor uav on se (3). In *Decision and Control (CDC), 2010 49th IEEE Conference on*, pages 5420–5425. IEEE, 2010.
- [15] Meier Lorenz, Honegger Dominik, and Pollefeys Marc. Px4: A node-based multithreaded open source robotics framework for deeply embedded platforms. In *IEEE International Conference on Robotics and Automation, ICRA'15*, pages 6235–6240, 06 2015.
- [16] A. Marcos and G. Balas. Development of linear parameter varying models for aircraft. *Journal of Guidance, Control and Dynamics*, 27:218–228, 2004.
- [17] Daniel Mellinger and Vijay Kumar. Minimum snap trajectory generation and control for quadrotors. In *Robotics and Automation (ICRA), 2011 IEEE International Conference on*, pages 2520–2525. IEEE, 2011.
- [18] Derek R Nelson, D Blake Barber, Timothy W McLain, and Randal W Beard. Vector field path following for miniature air vehicles. *IEEE Transactions on Robotics*, 23(3):519–529, 2007.
- [19] T Oliveira. *Moving Path Following Control System for Fixed-Wing Unmanned Aerial Vehicles*. PhD thesis, U. of Porto, Faculdade de Engenharia, April 2017.
- [20] Tiago Oliveira, A Pedro Aguiar, and Pedro Encarnação. Moving path following for unmanned aerial vehicles with applications to single and multiple target tracking problems. *IEEE Transactions on Robotics*, 32(5):1062–1078, 2016.
- [21] Sanghyuk Park, John Deyst, and Jonathan P How. A new nonlinear guidance logic for trajectory tracking. In *AIAA guidance, navigation, and control conference and exhibit*, pages 16–19, 2004.
- [22] Guilherme V Pelizer, Natássya BF da Silva, and Kalinka RLJ Branco. Comparison of 3d path-following algorithms for unmanned aerial vehicles. In *Unmanned Aircraft Systems (ICUAS), 2017 International Conference on*, pages 498–505. IEEE, 2017.
- [23] Daniele Pucci, Tarek Hamel, Pascal Morin, and Claude Samson. Non-linear feedback control of axisymmetric aerial vehicles. *Automatica*, 53:72–78, 2015.
- [24] Wei Ren and Randy W Beard. Trajectory tracking for unmanned air vehicles with velocity and heading rate constraints. *IEEE Transactions on Control Systems Technology*, 12(5):706–716, 2004.
- [25] Claude Samson. Path following and time-varying feedback stabilization of a wheeled mobile robot. In *Proceedings of the international conference on advanced robotics and computer vision*, volume 13, pages 1–1, 1992.
- [26] Lars Sonneveldt, ER Van Oort, QP Chu, and JA Mulder. Nonlinear adaptive trajectory control applied to an f-16 model. *Journal of Guidance, control, and Dynamics*, 32(1):25, 2009.
- [27] Brian L. Stevens and Frank L. Lewis. *Aircraft control and simulation*. Wiley-Interscience. J. Wiley and sons, New York, Chichester, Brisbane, 1992.
- [28] Jinni Zhou, Ximin Lyu, Zexiang Li, Shaojie Shen, and Fu Zhang. A unified control method for quadrotor tail-sitter uavs in all flight modes: Hover, transition, and level flight. In *Proc. of the IEEE/RSJ Intl. Conf. on Intell. Robots and Syst. IEEE*, 2017.